South America climate change revealed through climate indices projected by GCMs and Eta-RCM ensembles

Michelle Simões Reboita[1] · **Cassia Akemi Castro Kuki[1]** · **Vitor Hugo Marrafon[1]** · **Christie Andre de Souza[1]** ·
Glauber Willian S. Ferreira[1] · **Thales Teodoro[1]** · **José Wanderley Marangon Lima[2]**

Abstract
Studies that evaluate climate change projections over the whole of South America (SA) and including different seasons and models are scarce. In this context, the objective of this work is to assess climate projections for SA through the use of climatic indices, considering the entire continent, distinct seasons, and ensembles of models. Projections performed with the Eta regional climate model and its driving global climate models (GCMs) are analysed. From these projections, 19 climate indices based on daily precipitation and maximum and minimum temperature are computed. The results focus on two ensembles (GCMs and Eta), time slices (1980–2005 and 2050–2080), and scenarios (RCP4.5 and RCP8.5). In the validation of the present climate, it is shown that Eta adds value to GCMs. Future projections indicate, for both austral summer (DJF) and winter (JJA), an increase in the frequency and intensity of extreme events of daily rainfall over southeastern and extreme north of SA. Over the Amazon, during DJF, there is a statistically significant increase in the number of consecutive dry days and a decrease in the consecutive wet days. For northeastern Brazil, these features are more intense in JJA. The frequency of cold (warm) nights and days is projected to decrease (increase) over the whole continent and seasons. The climate change signal for the 19 climate indices is more intense under RCP8.5, and the regions more vulnerable to climate change are the Amazon, northeastern Brazil, and southeastern SA. Considering Brazil, the projections of precipitation and air temperature are also shown by biomes.

Keywords Climate projections · South America · Ensembles · Climate indices · Eta model · CORDEX · Biomes

1 Introduction

The average of weather events for an extended period characterizes the climate of a place (WMO 1983). When there is a change, be it in the average, in extreme values, or the shape of the frequency distribution, there is what is called climate change. Climate changes can be due to natural and/or anthropogenic causes (Hartmann 2016). With the beginning of the Industrial Revolution in the eighteenth century, the atmosphere chemistry composition began to be affected by the injection of greenhouse gases released during fossil fuel combustion. Historical time series of observed data have proven the changes in atmospheric composition and their impacts on the warming of the planet (IPCC 2007, 2013).

One consequence of climate change is the increase in extreme weather and climate events (Diffenbaugh et al. 2017; Ummenhofer and Meehl 2017). An extreme event is defined when a variable value is above or below a threshold obtained by applying statistical methods (IPCC 2012).

✉ Michelle Simões Reboita
reboita@unifei.edu.br

Cassia Akemi Castro Kuki
cassiakuki@yahoo.com.br

Vitor Hugo Marrafon
vitorhmarrafon@gmail.com

Christie Andre de Souza
christie@unifei.edu.br

Glauber Willian S. Ferreira
glauber_ferreira@unifei.edu.br

Thales Teodoro
thales.teo@hotmail.com

José Wanderley Marangon Lima
jose.marangon@marangonenergia.com.br

[1] Universidade Federal de Itajubá, Itajubá, MG, Brazil

[2] Marangon Consultoria e Engenharia, Itajubá, MG, Brazil

An example of an extreme climate event is the increase of consecutive days without precipitation in a given region. An illustration of extreme weather events happens when a very voluminous rainfall amount occurs in a short period within a day. Besides, extreme events can be considered in terms of their frequency, intensity, duration and the damage caused (Beniston and Stephenson 2004; Seneviratne et al. 2012). For simplicity, extreme weather and climate events are called extreme events only.

The identification of extreme events and their intensity and duration is carried out using indices defined in the literature (Alexander et al. 2019). The CCl/CLIVAR/JCOMM Expert Team (ET) on Climate Change Detection and Indices (ETCCDI; http://etccdi.pacificclimate.org/) has developed 27 climate indices to help the characterization of climate variability and climate changes. It is also possible to intercompare results when the indices are calculated with different datasets and in distinct regions of the globe. These indices are based on daily precipitation, minimum and maximum temperature data.

While there is a substantial number of studies available on extreme events in South America (SA) for the present climate (e.g., Haylock et al. 2006; Skansi et al. 2013; Donat et al. 2013a; Rao et al. 2016; Rusticicci et al. 2016; Marrafon and Reboita 2020; Dereczynski et al. 2020; Céron et al. 2020; Marengo et al. 2020; Dunn et al. 2020), the same does not occur for the future climate (e.g., López-Franca et al. 2016; Lyra et al. 2018; Reboita et al. 2018; Blázquez and Solman 2020; Li et al. 2020). Moreover, few studies address the features of extreme events by season, considering the whole South American continent in the climate projections.

In terms of the present climate, some studies have indicated a decrease (increase) in the number of cold (warm) days and nights since 1950 (IPCC 2013; Dereczynski et al. 2020; Dunn et al. 2020). Globally, the trends observed in air temperature show a clear sign of an increase in all seasons, which does not occur with precipitation since this variable presents different signals depending on the region (IPCC 2013). For example, Marrafon and Reboita (2020) calculated the trends of different precipitation indices using data from the Climate Prediction Center (CPC) from 1979 to 2019. In general, there is a trend to reduce the seasonal and annual volume of rainfall in most part of Brazil. The authors also found a decrease (increase) trend in the sequence of wet days (dry days). Among southern Paraguay, northeastern Argentina, part of southern Brazil, and Uruguay (a region known as southeastern SA), the climate indices either show no trend or indicate an increase in wet conditions (Skansi et al. 2013; Lovino et al. 2018). Dereczynski et al. (2020) evaluated the performance of three simulations of the Eta regional climate model (20 km; which is an integrant from the Coordinated Regional Climate Downscaling Experiment-CORDEX; Gutowski et al. 2016) in the period 1965–2005. The

authors made comparisons between some climate indices obtained in the simulations and observed data. Eta nested in CanESM2 shows the most prominent temperature trends among the three simulations. Furthermore, Eta nested in MIROC5 simulates better the signal and magnitude of the extreme temperature trends. Eta-MIROC5 also presents the best simulations in terms of precipitation trends, showing an increase in the magnitude of the precipitation extremes over most of SA.

For the future climate, Reboita et al. (2014a) and Llopart et al. (2020a, b) show an increase in temperature with prominence in the Amazon Basin. A rainfall deficit is also projected in this same basin, considering the period 2070–2100 and the Representative Concentration Pathway 8.5 (RCP8.5) scenario. For the La Plata Basin, these studies project an increasing trend both in temperature and rainfall towards the end of the twenty-first century. Blázquez and Solman (2020) analysed extreme events projected by a set of Regional Climate Models (RCMs) from CORDEX (including Eta model) and their driving GCMs from the Coupled Model Intercomparison Project (CMIP5). The periods of the study were 1979–2005 and 2071–2100, considering the RCP4.5 scenario. Among the results, the authors highlighted the increase of extreme precipitation events over the subtropics with a robust signal among models. On the other hand, for tropical latitudes, they found a high dispersion among the projections.

Given the preceding, the objective of this study is to present climate projections for SA based on a selection of ETCCDI indices applied to projections of GCMs and RCM (in this case, the Eta model). We focus on two scenarios (RCP4.5 and RCP8.5) and time slices: present (1980–2005) and future (2050–2080). Furthermore, this work attends to the Brazillian Ministry of Mines and Energy (MME) request in the context of the project "Climate study: Analysis of the Vulnerability of Hydroelectric Plants to the Impacts of Climate Change". This study is in line with the World Climate Research Program (WCRP; wcrp-climate.org) and CORDEX project. Moreover, the present work serves as a decision-makers tool to establish adaptation and mitigation measures in the face of climate change.

2 Methodology

2.1 Study area

The study area is South America (Fig. 1), which extends from 55°S to 12°N and covers areas in the extratropical, subtropical, and tropical latitudes (Reboita et al. 2010). The highest topography of SA is the Andes mountains, which cover about 8.850 km along the continent's western edge. The other two highland areas in SA are the Brazilian
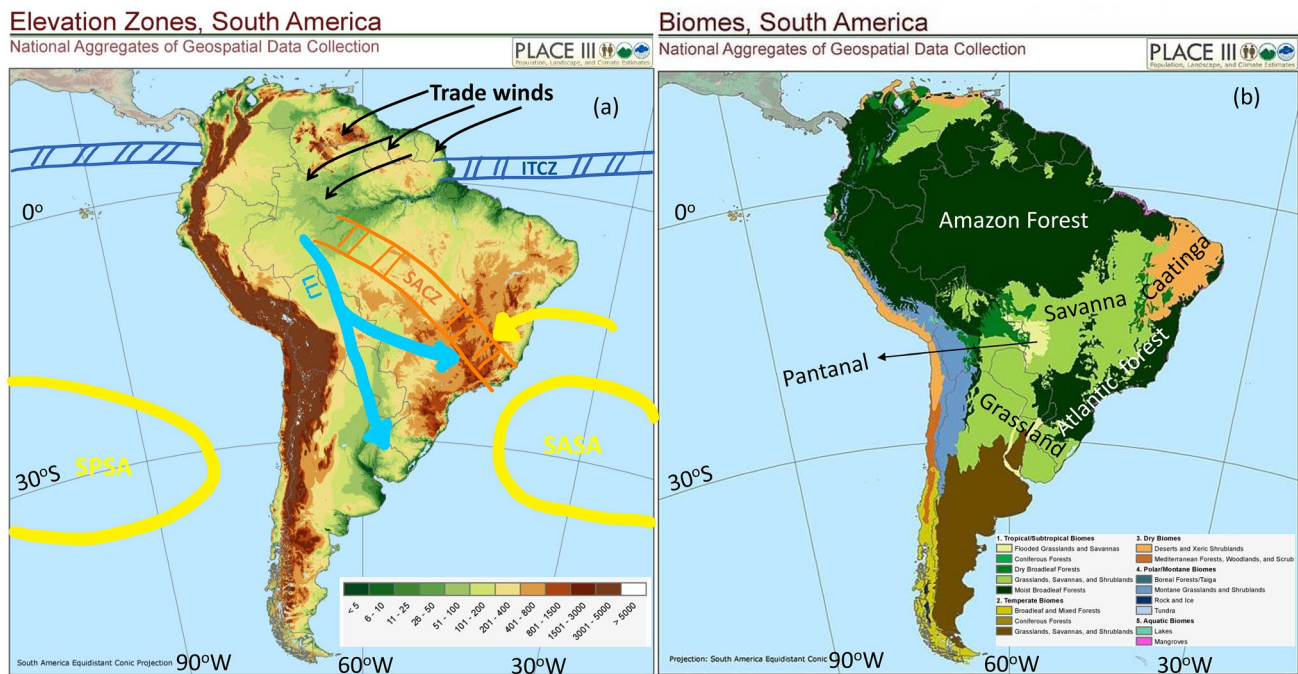
Fig. 1 South America **a** topography (meters) and main atmospheric systems at lower levels during the rainy season and **b** biomes. ITCZ means Intertropical Convergence Zone, LLJ is the low-level jet eastern the Andes, SACZ is the South Atlantic Convergence Zone, and SPSA and SASA are the South Pacific Subtropical Anticyclone and South Atlantic Subtropical Anticyclone, respectively. Adapted from Earth Observing System Data and Information System (EOSDIS) of NASA—Socioeconomic Data and Applications Center (SEDAC) (https://sedac.ciesin.columbia.edu/data/set/nagdc-population-landscape-climate-estimates-v3/maps?facets=region:south%20america)

Highlands (south and southeastern Brazil) and the Guiana Highlands (Fig. 1a). SA is the place of two crucial river basins: Amazon (located in the centre-northwestern SA) and La Plata (located in southeastern SA and covering areas of southeastern Bolivia, southern and central Brazil, the entire country of Paraguay, most of Uruguay, and northern Argentina) (National Geographic 2020). Regarding the biomes, tropical forests cover most of the continent (Fig. 1b). The Amazon Forest is located in the centre-northwest part of SA, while the Atlantic Forest extends along the Atlantic coast of Brazil. Savanna biome is found in the central part of Brazil ("Cerrado" is the local name). Among Paraguay, Argentina, Uruguay and southern Brazil, the grassland is locally called Pampas. In the semi-arid region of SA (northeast Brazil), the dominant biome is the Caatinga, arid shrubland. Pantanal, which is the world's largest freshwater wetland (Calheiros et al. 2012), is located among the Brazilian states of Mato Grosso and Mato Grosso do Sul (~ 80%), with minor shares in Bolivia (~ 19%) and Paraguay (~ 1%).

Most SA is characterized by a monsoon climate, with a predominance of well-defined dry and wet seasons. Details about the SA monsoon can be found in Zhou and Lau (1998), Vera et al. (2006), Reboita et al. (2010, 2014a), Marengo et al. (2012) and Ashfaq et al. (2020). The wet season occurs from October to March, with a peak in austral summer (DJF). Figure 1a depicts some of the central atmospheric

systems at lower levels that contribute to precipitation in this period. The South Atlantic Convergence Zone (SACZ) is a crucial system for precipitation in large parts of Brazil. This system is characterized by a band of clouds and precipitation that extends from the southern Amazon to southeastern Brazil and reaches the Atlantic Ocean (Carvalho et al. 2004; Silva et al. 2019a; Escobar and Reboita 2020). Its development occurs through the association of different atmospheric mechanisms. One process is the combination of local convection with the moisture transported to the subtropics from the Amazon, by the low-level jet (LLJ) eastern of the Andes (Santos and Reboita 2018; Montini et al. 2019), and from the South Atlantic Ocean, by the northwestern winds of the South Atlantic Subtropical Anticyclone (Reboita et al. 2019).

2.2 Data

Daily precipitation, minimum and maximum temperature data of the Climate Prediction Center (CPC, https://www.esrl.noaa.gov/psd/data/gridded/data.cpc.globalprecip.html), from the period 1980–2005, are used. These data cover the globe with 0.5° horizontal resolution and are generated by interpolating information measured in meteorological stations (Chen et al. 2008).

2.3 Climate projections

This work uses climate projections from GCMs and the Eta regional model (Mesinger et al. 2012). The GCMs used are Canadian Earth System Model (CanESM2; Chylek et al. 2011; Arora et al. 2011), Hadley Center Global Environmental Model—Earth System (HadGEM2-ES; Collins et al. 2011; Martin et al. 2011) and Model for Interdisciplinary Research on Climate version 5 (MIROC5; Watanabe et al. 2010). The projections of these models were obtained from the Earth System Grid Federation (ESGF; https://esgf-node.llnl.gov/search/cmip5) platform. The Eta regional climate model (Pesquero et al. 2010; Chou et al. 2012; Mesinger et al. 2012) was nested in the outputs of these three GCMs, as well as to the Brazilian Earth System Model (BESM) outputs since they can represent the characteristics of atmospheric circulation adequately in SA (Chou et al. 2014a, b). The downscaling technique is important to improve climate representation by including regional aspects of the atmospheric circulation (Ambrizzi et al. 2019). Eta was integrated with 20 km of grid-space in a domain covering SA and adjacent oceans; details of the physical parameterizations used in the projections are provided in Dereczynski et al. (2020). Here the projections of the three GCMs (CanEMS2, HadGEM2-ES and MIROC5) and the four downscaling projections of Eta are analysed. Eta projections were obtained directly from Dr. Chou Sin Chan (responsible researcher for the Eta model in Brazil) since not all variables are available on the ESGF platform. BESM was not included in the ensemble of the GCMs because it was not available.

Two time slices and two climate scenarios (RCP4.5 and RCP8.5) are analysed. The first time slice corresponds to the present climate (1980–2005). The authors considered this period due to: (a) avoiding missing data or low density of meteorological stations in most areas of Brazil (Xavier et al. 2015; Sun et al. 2017), and (b) 2005 is the last year of the CMIP5 simulations without the inclusion of the scenarios of the greenhouse gases emissions (Taylor et al. 2012; Xiao-Ge et al. 2013). For the future climate, the analysed period is 2050–2080 due to a request of the MME-Brazil. Although the historical period has 26 years and the future 31 years, this difference does not affect the comparisons between them since the study focuses on averages (e.g., Shafiq et al. 2019). RCP indicates the changes in radiative forcing and the value reached in the year 2100 associated with the concentration of greenhouse gases in the atmosphere. Changes in radiative forcing (W m^{-2}) come from greenhouse gas emissions, pollutant emissions, and land use and coverage (https://ar5-syr.ipcc.ch/topic_futurechanges.php). The intermediate RCP4.5 scenario has a peak of emissions in 2040, followed by a decline. In 2100 the radiative forcing is 4.5 W m^{-2}. The RCP8.5 scenario is the most pessimistic, with a radiative forcing of 8.5 W m^{-2} in 2100 (Moss et al. 2010; van Vuuren

et al. 2011; Taylor et al. 2012). Both scenarios are considered in this study.

The GCMs used in this study have different spatial resolutions. GCM simulations can be interpolated for a common grid for intercomparison, which varies between $1° \times 1°$ to $2° \times 2°$ (Santos et al. 2017; Khan et al. 2020). For this study, we chose to interpolate all GCM simulations for a grid with a spacing of $1.5°$ (~150 km) with the bi-linear technique (Schowengerdt 2007; Li et al. 2019), which is a standard procedure (Chen and Knutson 2008). The Eta model was maintained in its original 20 km grid.

2.4 Extreme climate indices

Although ETCCDI presents 27 extreme climate indices, in this study, only 14 indices are calculated since they address the main questions of MME about the climate indicators of impacts on the Brazilian Electrical System from 2050 to 2080. Moreover, some ETCCDI indices do not have definitions appropriate to be used in the study area (Ávila-Diaz et al. 2020). The calculated indices provide the intensity, frequency and duration of extreme climate events. As the ETCCDI indices are widely known (Frich et al. 2002; Alexander et al. 2006; Klein Tank et al. 2009; Zhang et al. 2011; Donat et al. 2013b; Sillmann et al. 2013; Dunn et al. 2020), here we present only the name of the calculated indices (Table S1 presents a complete description of them). Based on daily precipitation accumulation, total precipitation (PRCTOT), very wet days (R95p), consecutive dry days (CDD) and consecutive wet days (CWD) are calculated. By using minimum and maximum daily temperatures, the indices calculated are the mean of the minimum and maximum temperatures (TN and TX), the minimum value of the daily minimum and maximum temperatures (TNn and TXn), the maximum value of the daily minimum and maximum temperatures (TNx and TXx), cold nights (TN10p), warm nights (TN90p), cold days (TX10p) and warm days (TX90p).

The indices are calculated for each season (summer-DJF, autumn-MAM, winter-JJA and spring-SON). In the present climate, as the study period is from 1980 to 2005, there are 26 seasons (for example, 26 summers). For the future period, there are 31 seasons. This difference in the length of the time series does not affect the comparisons between the periods since we are focusing on averages. In addition to the extreme climate indices, the seasonal averages of the mean temperature are calculated, with the daily mean temperature defined following WMO (1983): (minimum temperature + maximum temperature)/2.

The trends in the climate indices are also evaluated. The trend is calculated with the simple linear regression method (Mudelsee 2019) while the statistical significance is obtained with the Student t test (Wilks 2011) and considering $\alpha = 0.1$ (90% confidence). Although the time series

of the historical period have 26 years (which is shorter than the 30-year period recommended in climate studies), it is enough length to detect the trend signal since it can even be obtained with time series shorter than the 20-year period (Lang et al. 2019). When the mean time series of a given index is presented on a map, hatchings indicate the regions with a statistically significant trend. Significant positive trends in red (blue) refer to an increase (decrease) in the temperature or decrease (increase) in the rain. For instance, in the PRCTOT, CWD, TN10P, TX10P, TXn, TNn and R95p indices, the positive trends appear in blue. The positive trends appear in red in the TX90p, TN90p, CDD, TNx and TXx indices.

The extreme climate indices were computed by model, projection, and time slice. Afterward, we computed the ensembles of the indices for GCMs and Eta.

2.5 Analyses

The climate indices were computed for DJF and JJA, and we focus only on ensemble mean (and not on the individual members of the models). One reason for this is that the ensemble averages or medians are often better at reproducing observations than even the best individual model (e.g., Tebaldi and Knutti 2007; Hagemann and Jacob 2007; Leutbecher and Palmer 2008; IPCC 2010; Parker 2013; Martre et al. 2015; Wallach et al. 2016; Lee et al. 2020).

The ensembles' mean performance (hereafter called ensembles for brevity) in simulating the historical period is evaluated through comparisons with CPC. In the sequence, climate change signals in the different climate indices (Table S1) are presented. The statistical significance of the projected climate changes (future–present) is calculated by a two-sample t test for difference of means (Zhang et al. 2005; Wilks 2011; Montgomery et al. 2015) and considering $\alpha = 0.1$ (90% confidence). Finally, a summary of the climate change in the main Brazilian biomes is shown.

3 Results

3.1 Present climate

This section presents the validation of Eta and GCMs ensembles in the present climate (1980–2005). This analysis allows identifying the ensembles' ability to reproduce the main characteristics of the South American climate. For brevity, only five indices (Table S1) are discussed here: PRCTOT, P95, R95p, CDD, and TMED. While PRCTOT and TMED describe the mean state of the climate, R95p and CDD are considered key indicators for monitoring changes in climate extremes (Peterson et al. 2001). Besides being a meaningful threshold for daily precipitation extremes, P95

is used to calculate R95p (details in Table S1). Although GCMs and Eta ensembles have satisfying performance in representing the spatial precipitation pattern in the wet (DJF, Fig. 2a–c) and dry (JJA, Fig. 3a–c) periods of SA monsoon compared with CPC, they present some differences in the rainfall volume. Considering DJF (Fig. 2a–c), the ensembles underestimate the precipitation over the Amazon. Also, they displace the maximum precipitation located in the south of that region in CPC to the midwest and southeast of Brazil. These features are also documented in the validations performed by Chou et al. (2014a, b). In JJA (Fig. 3a, b), precipitation is scarce in a large part of the continent compared with DJF. The highest totals are found in the extreme north of SA, associated with the ITCZ (Reboita et al. 2010), followed by southern Brazil, associated with the influence of the synoptic systems (fronts and cyclones; Blázquez and Solman 2019; Reboita et al. 2010, 2020). Ensembles have some differences compared to CPC. For instance, GCMs underestimate the precipitation in the extreme north of SA and southern Brazil. Besides, Eta displaces the maximum precipitation found in north SA and simulates wetter conditions over the Amazon and drier conditions in a large area of Argentina.

In terms of statistically significant trends in PRCTOT, CPC shows in DJF negative trends over the Amazon, Bolivia, and in some areas southern 20°S over Chile and Argentina (Fig. 2a). In JJA, practically, there are no trends in those areas, but a negative trend appears over the centre of Brazil (Fig. 2a). These results agree with Marrafon and Reboita (2020) that evaluated the seasonal trends in a more extended period (1979–2019) of CPC. Moreover, the results agree with studies that used station data (Skansi et al. 2013; Dereczynski et al. 2020) or grid point datasets (Ávila-Diaz et al. 2020) to perform an analysis of the annual trend. In general, those authors show for PRCTOT, when the four seasons are considered (figures not shown), significant negative trends over a large part of the central-south Amazon, Bolivia, and in parts of the centre and northeast Brazil, and positive and significant trends over the south of Brazil, Uruguay and in sparse areas of other sectors of La Plata Basin. Considering the ensembles, they do not represent these trends satisfyingly. For example, in DJF, while GCMs only show a positive trend over central Argentina, Eta indicates a large area of the continent with a positive trend (Fig. 2a–c). However, in a general view, Eta adds value to the GCMs. For instance, Eta corrects the overestimation of precipitation over the Andes in DJF and reproduces the maximum precipitation values in JJA registered by CPC over southern Brazil.

To study the extreme precipitation events, initially, the 95th percentile (P95) of the daily time series is calculated. This value is shown in Figs. 2 and 3d–f, and it reveals that daily extremes are more intense and cover a larger area in the CPC than in the ensembles. For instance, in DJF in the La Plata Basin, P95 exceeds 45 mm day^{-1} in CPC, while in

Fig. 2 DJF climate indices for the historical period (1980–2005) from CPC (left), GCMs ensemble (middle) and Eta ensemble (right): **a–c** precipitation (PRCTOT, mm), **d–f** 95th percentile (P95, mm), **g–i** number of days in that the daily precipitation exceeds P95 (R95p, days), **j–l** consecutive dry days (CDD, days), and **m–o** mean air temperature (TMED, °C). Cross-hatching regions indicate a significant trend. For PRCTOT and R95p blue (red) indicates positive (negative) trends and for CDD and TMED blue (red) indicates negative (positive) trends
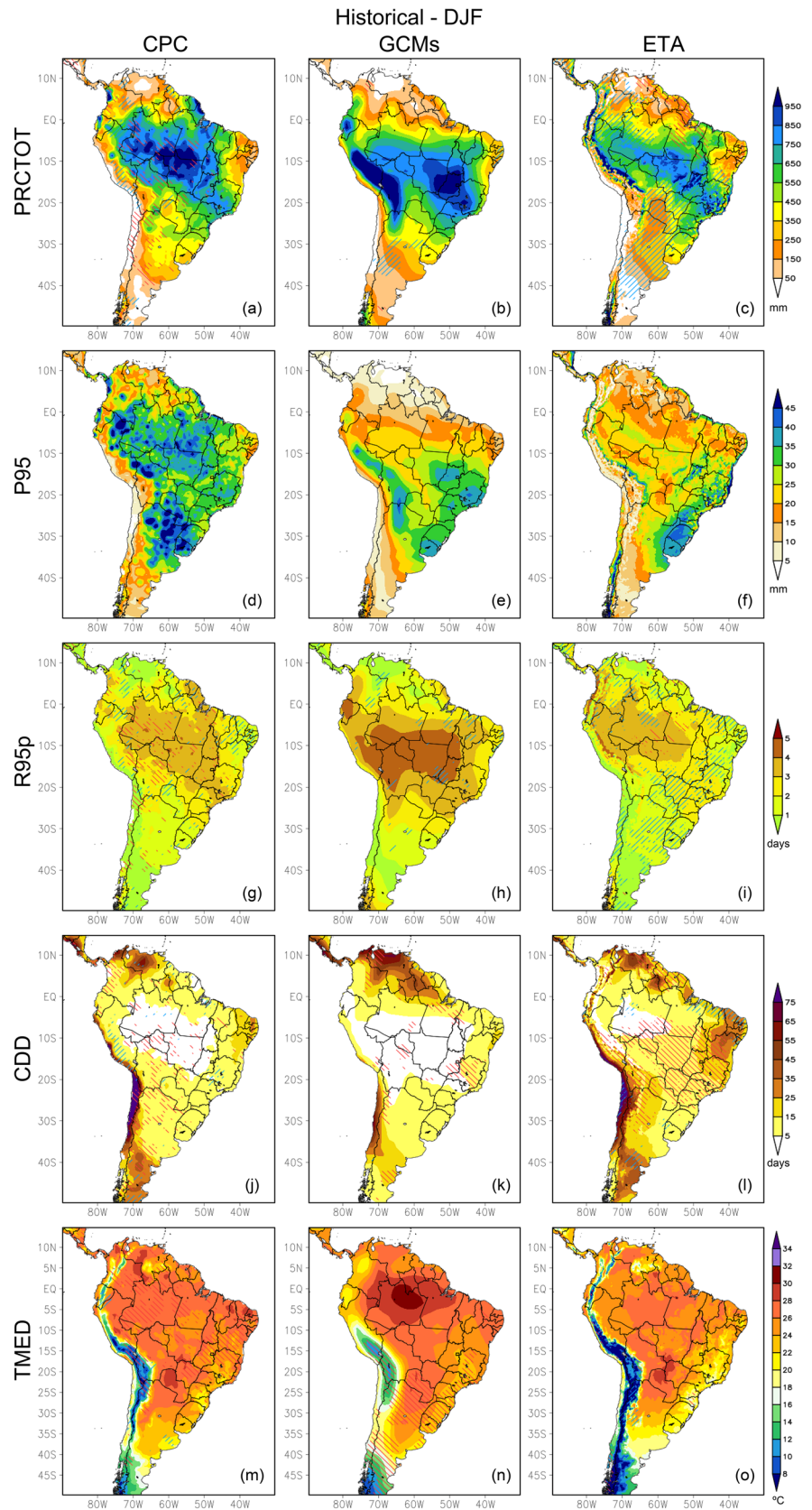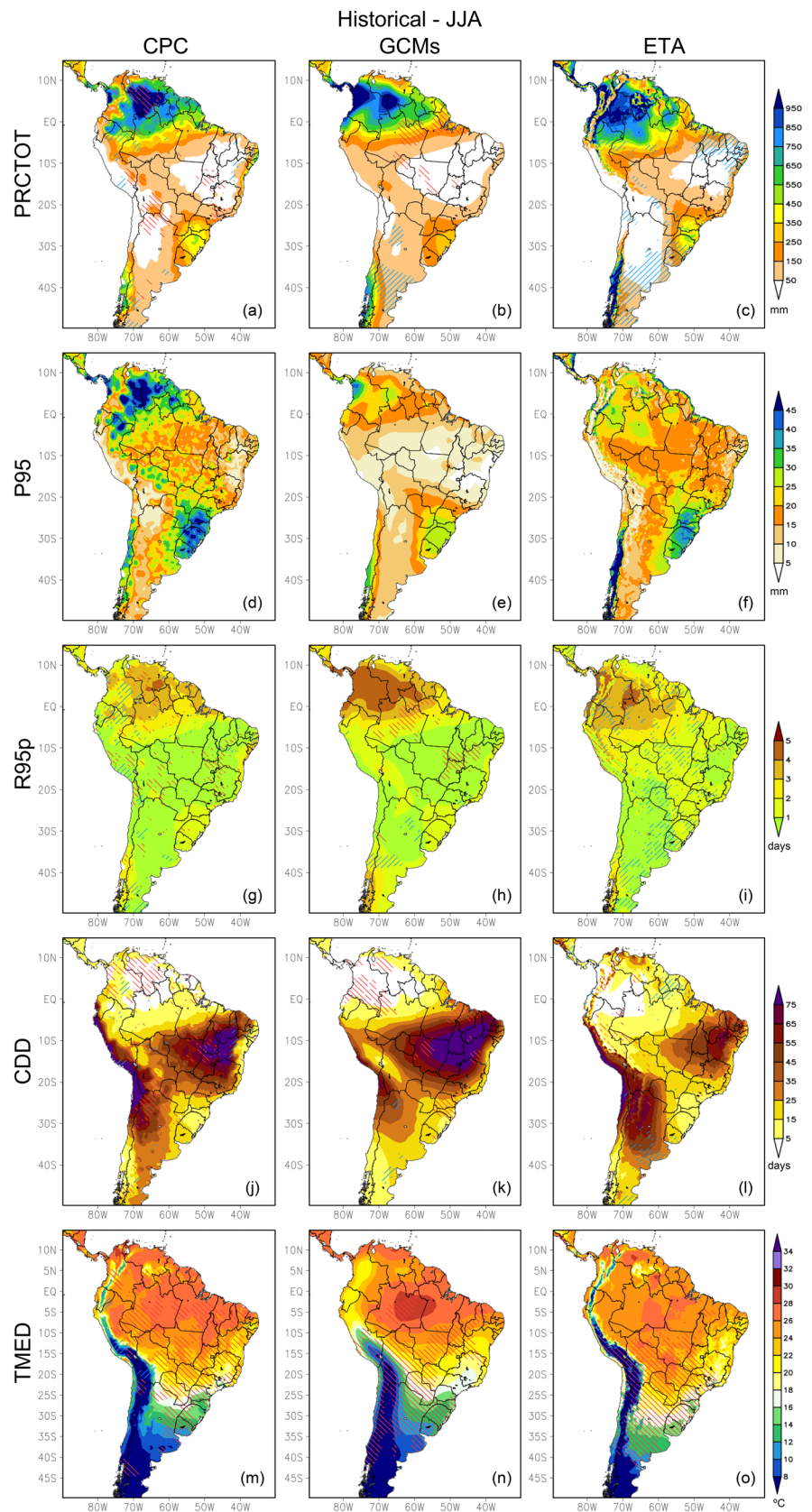
Fig. 3 Similar to Fig. 2 but for JJA

Historical - JJA

GCMs (Eta), it is ~ 30 (~ 40) mm day^{-1}. As the underestimation of Eta is lower than that of GCMs, it adds value to the global models (Fig. 2d–f). As in Chou et al. (2014a), BESM and MIROC5 models significantly contribute to dry conditions in the Eta ensemble (figures not shown). In JJA, CPC shows higher values of P95 in the extreme north of SA, southern Brazil and Uruguay. Although both ensembles underestimate P95 in these regions, Eta simulates P95 closer to CPC over southern Brazil and Uruguay (Fig. 3d–f). Since the percentile is a single seasonal value obtained over the time series, there is no way to compute the trend of this variable.

When the time series have the same length, a specific percentile will correspond to the same number of occurrences in all grid points. However, it is not the case for the extremes of precipitation. For calculating the percentile of precipitation (95%), days without rainfall are excluded from the time series (e.g. Boroneant et al. 2006). Consequently, each grid point will have a daily precipitation time series with a different length, which implies in a different number of extreme events corresponding to the 5% percentile. Then, we show the average seasonal number of days, here called R95p, in which rainfall is higher than the P95 threshold (Figs. 2g–i, 3g–i), and not the sum of the precipitation in the extreme days, which is called R95pTOT by the ETC-CDI (http://etccdi.pacificclimate.org/list_27_indices.shtml). In DJF, the spatial pattern of Eta is very similar to that of CPC (Fig. 2g–i). However, there is an underestimation in the number of days with extreme events in the central-west and southeastern Brazilian regions. Between 20° and 10°S, GCMs simulate a large area with the number of days exceeding that from CPC. In JJA (Fig. 3g–i), Eta overestimates the number of days with extreme precipitation from the Amazon to southern Brazil while GCMs overestimate it in the north of SA. Considering the trend in DJF, CPC shows negative and significant trends along the SACZ, Bolivia, Chile and in some sparse areas of Argentina, indicating a decrease in the frequency of the extreme daily events of precipitation. On the other hand, there is a positive and significant trend over northeast and south of Brazil, Paraguay and Uruguay (Fig. 2g). Eta and GCMs have low performance in reproducing the trends (Fig. 2h, i), while Eta almost does not show trends in DJF over SA, GCMs ensemble simulates positive trends over almost the whole SA (except in Peru, Amazon and central Brazil). In JJA, CPC indicates negative and significant trends over west SA and some northeast and southeast Brazil parts. Eta has more similarities with CPC in this season, while GCMs continue indicating positive trends over a large portion of the continent (Fig. 3g–i). CPC trends can be compared directly with Marrafon and Reboita (2020) but not with the other authors mentioned across the text (e.g., Soares et al. 2016; Ávila-Diaz et al. 2020) since they show the trend of the accumulated precipitation during

the extremes and not their frequency. A fact that deserves attention is that the spatial pattern of the trends indicated by CPC for the extreme frequency is in remarkable agreement with the interpolated station data presented by Ávila-Diaz et al. (2020) for the accumulated precipitation. However, both datasets have a distinct spatial pattern from ERA5 and two merged products with satellite estimates from 1980 to 2016 (also shown in Ávila-Diaz et al. 2020). This fact reveals that the datasets used for model validations also have uncertainties and they need to be stressed in the studies. One of the uncertainties stems from the observations being collected from rain gauges or weather stations. Given that the meteorological station density varies around the globe (Rozante et al. 2010; Xavier et al. 2015), observations for regions with a low density of stations, such as the Amazon Basin, may have their interpolation quality reduced (Ávila-Diaz et al. 2020). The uncertainties of the datasets used to validate models are also shown by Soares et al. (2016).

Figures 2a–c and 3a–c show that, in general, the ensembles underestimate the precipitation compared to CPC. This feature can be a reason for the higher average number of CDD in the models (Figs. 2j–l, 3j–l). In DJF, from Bolivia to northern Argentina and in sparse areas of the northeast of Brazil, the datasets show a positive trend of CDD. Differently, over a part of southeast Brazil, there is a decrease in CPC and an increase in ensembles. While in DJF (Fig. 2j–l), the highest frequency of CDD is registered along the extreme regions of SA (north and south borders and over the Andes), in JJA (Fig. 3j–l), it occurs in most of the continent (central, southeast and the northeast regions of Brazil, Andes and Argentina). In JJA, Eta underestimates the CDD in the northeastern semi-arid region and overestimates it in Argentina's large area. The opposite occurs for the GCMs. In this season, Eta gets to represent the positive trend over northern Argentina, resembling CPC. The trend signals showed in Figs. 2j–l and 3j–l agree with those studies that performed an annual analysis and indicate CDD significant positive trends over the central, southeast and northeast regions of Brazil and along the Andes from Bolivia to Argentina (Skansi et al. 2013; Ávila-Diaz et al. 2020; Dereczynski et al. 2020). Trends signal in CDD, in general, is opposite to that from CWD (figures not shown). In DJF, CPC shows a decrease in CWD between the north and centre of Brazil and in a vast area of Argentina. Eta simulates the decrease over Brazil but shows a positive trend as GCMs over Argentina. The trends registered in CDD and CWD obtained from CPC also agree with a more extended CPC time series (Marrafon and Reboita 2020).

In terms of seasonal mean temperature (TMED), in both DJF and JJA (Figs. 2m–o, 3m–o), northward 10°S GCMs are warmer, and Eta is colder than CPC. Despite that, in the extreme south of SA, Eta is slightly warmer than CPC. For the trends, in DJF (Figs. 2m–o), CPC shows a significant

positive trend dominating north of 25°S (except over the Andrean countries), which agrees with the trends obtained for this same season in the CRU dataset from 1975 to 2004 in Soares et al. (2016). Ensembles do not have a good skill in simulating the DJF trends since GCMs show positive trends south of 20°S and Eta does not indicate significant trends over the whole continent (except for the negative ones over the Andes). In JJA, as in Soares et al. (2016), the significant positive trends occur in almost the whole continent, except in portions of Peru, Bolivia and Argentina. Ensembles simulated the positive trends between 35° and 5°S but included the areas without significant trends in CPC. Concerning the mean maximum temperature, TX (figures not shown), Eta adds value to GCMs since it reduces the warm bias mainly in DJF over Paraguay and adjacent regions showing values closer to CPC. It is a satisfying performance of Eta because most RCMs overestimate the air temperature over Paraguay and neighbourhood (Reboita et al. 2014a; Ambrizzi et al. 2019). For the mean minimum temperature, TN (figures not shown), Eta also has better performance in simulating the seasonal pattern and magnitude of this variable over SA since it reduces the warm bias of the GCMs mainly over the Amazon.

The discussion about the Eta and GCMs ensembles individual members' performance is beyond the goal of this study. Nevertheless, to support the view that Eta adds value to the GCMs and that there is a spread among the simulations, we show the individual members only for PRCTOT and CDD in DJF (Figs. S1 and S2). A discussion about the performance of the individual members of Eta is provided in other studies, such as in Chou et al. (2014a) for minimum and maximum temperature and in Almagro et al. (2020) for precipitation (considering Eta-HadGEM2-ES and Eta-MIROC5 over Brazil). For PRCTOT (Fig. S1), MIROC5 overestimates the precipitation over the Andes and in a wide band from the Amazon to the southeast/northeast Brazil, while CanESM2 underestimates the precipitation in these areas and in the extreme north of SA. HadGEM2-ES shows better performance among the GCMs. Comparing the individual members of the Eta ensemble with its driving GCMs, we can verify a great added value by Eta simulations since this RCM tends to correct the excessive wet/dry bias of the GCMs (Fig. S1). For CDD, GCMs individual members underestimate this index over a large area of central Brazil and overestimate it in the extreme north of SA. Again, Eta members improve the GCMs simulation of the spatial distribution and values of CDD (Fig. S2).

The ensembles shown in Figs. 2 and 3 and the individual members in Figs. S1 and S2 indicate a better performance of Eta compared to GCMs. Although Eta and GCMs ensemble has some differences in terms of intensity and trends compared with CPC, in general, they reproduce the main characteristics of the South American climate and, for this reason, they can be applied in future climate studies. Furthermore, differences in intensity of the ensembles with CPC are not a big issue because our interest is in the projected change signal obtained from the difference between future projections and the historical period.

3.2 Future climate

This section presents the future climate projections for the climate indices, shown in Table S1, under RCP4.5 and RCP8.5 scenarios and DJF and JJA seasons. The climate change signal is defined as the difference between the 2050–2080 and 1980–2005 periods.

3.2.1 Precipitation

The considerable concern on the future climate is associated with two aspects. The first point is the accumulated seasonal precipitation since it is crucial to the water supply for life, irrigation, energy generation and other activities. The other aspect is related to extreme daily rainfall events. The increase in frequency and intensity of these extremes can cause major troubles in urban centres, such as flooding, landslides and public health problems. Then, we start focusing on these variables.

PRCTOT: In DJF (Fig. 4a–d), both ensembles and scenarios indicate a statistically significant increase (decrease) of precipitation over southeastern SA (over a large area including the Amazon and north SA). Under RCP8.5, these climate change signals are more intense than under RCP4.5. The difference between the ensembles occurs over southeastern Brazil, evidencing that while Eta ensemble projects dry conditions over the whole SACZ, GCMs show wet conditions over the southeast. Chou et al. (2014b), using only HadGEM2-ES and MIROC5 models nested in Eta, also project dry conditions over SACZ with great intensity over southeast Brazil. In JJA (Fig. 5a–d), under RCP4.5, the GCMs project significant wet conditions in an extensive band in the west part of SA from the Equator to Argentina. They also present statistically significant wet conditions between southern Brazil and the south of the southeast Brazilian region. Eta shows a less extensive area with these features than GCMs, and over Brazil, the wet conditions have more intensity around 25°S. In RCP8.5, the area with positive trends is reduced. For this scenario, dry conditions dominate over the continent, having more intensity in the north of SA and southern Chile. GCMs differ from Eta since they project a drier climate between Paraguay and southern Brazil.

The climate change signals projected by the GCMs ensemble are in line with Llopart et al. (2020a), although these authors do not use the same models from here. On the other hand, the Eta ensemble diverges from other RCMs in
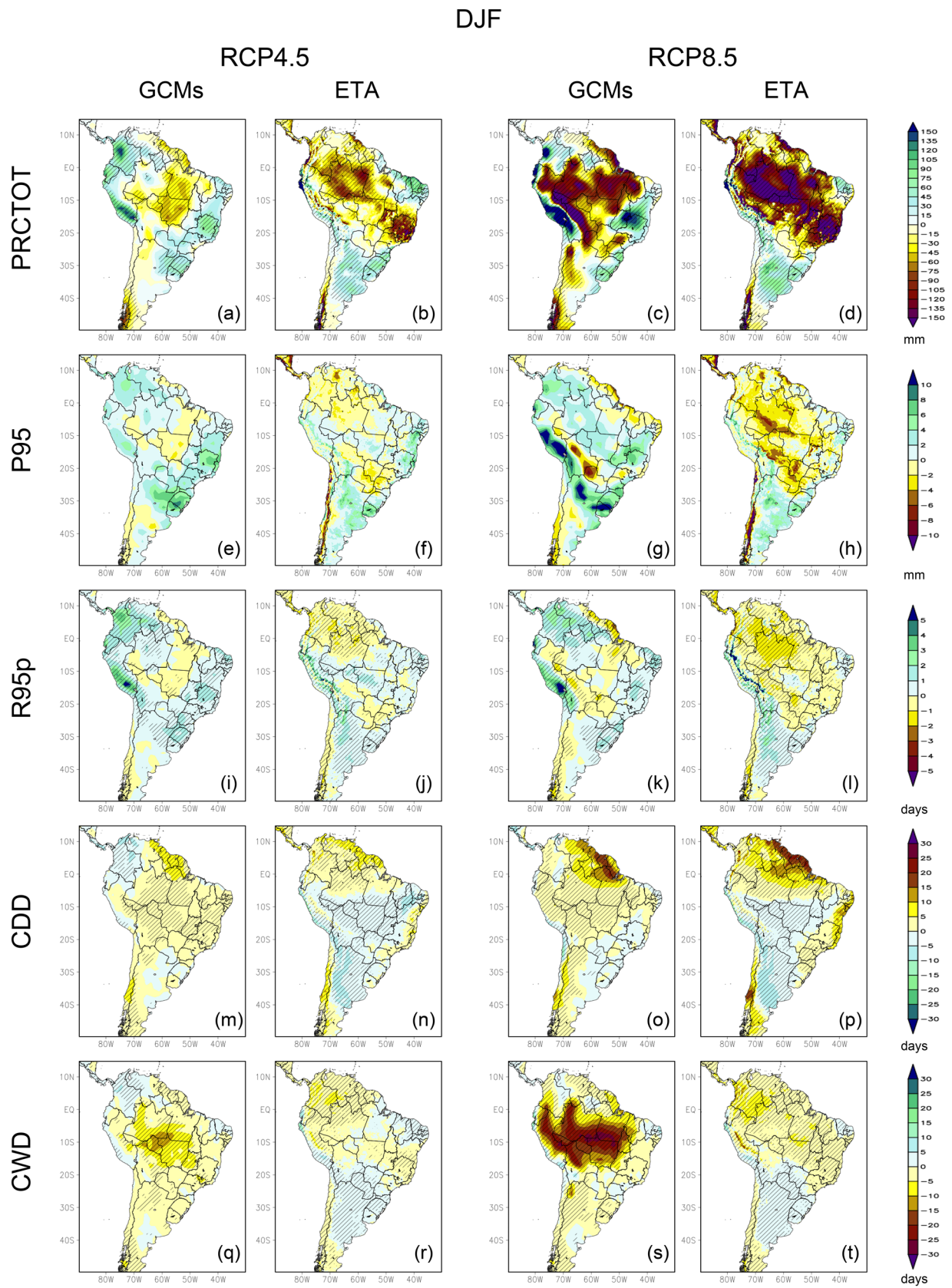
◀ **Fig. 4** Changes (future minus present) projected to the precipitation climate indices from GCMs and Eta ensembles in DJF: **a–d** PRC-TOT (mm), **e–h** P95 (mm), **i–l** R95p (days), **m–p** CDD (days) and **q–t** CWD (days). From left to right: GCMs and Eta ensembles under RCP4.5 and RCP8.5, respectively. Cross-hatching presents differences statistically significant at 0.1 confidence level

DJF, such as RegCM. While Eta projects a negative trend of precipitation over southeastern Brazil under RCP4.5 and RCP8.5, RegCM follows the GCMs signal, indicating wetter conditions (Llopart et al. 2020a; b). The physical explanation of these differences is beyond the scope of this study. Despite that, we suggest that the distinct physical parameterizations used in RCMs may lead to different trends in precipitation (Reboita et al. 2014b). These comparisons make clear the uncertainties associated with climate projections.

The literature has some indications concerning the physical explanation for the dry conditions projected over the Amazon and north of SA under both scenarios. One example is in Fig. 5 from Ambrizzi et al. (2019), a study that presents a synthesis of different RCMs projections. The figure indicates that the projected precipitation deficit is associated with the northeastern trade winds weakening at the end of the twenty-first century (2070–2100). This feature leads to a decrease in moisture transport from the ocean to the continent. Recently Llopart et al. (2020b) also attributed the decrease of precipitation in the Amazon Basin to the weakening of the large-scale moisture flux convergence. Dry conditions over the Amazon can further disturb the climate of other regions that receive tropical moisture transported by the LLJ eastern of the Andes. It may be one reason for the dry conditions projected by the Eta ensemble over southeastern Brazil. Otherwise, it also suggests that the precipitation over southeastern SA is not affected by the Amazonian conditions since the models project wet conditions. Over this region, Llopart et al. (2020b) showed large-scale flux convergence proceeding from the Atlantic Ocean.

We would also like to highlight that the trends in the PRCTOT do not have a linear answer to the increase of the greenhouse gases as the air temperature (as we show in the following sections). Although the Clausius-Clapeyron relationship predicts an increase in the water holding capacity of air of approximately 7% per degree Celsius rise in temperature (Held and Soden 2006; Skliris et al. 2016), which may lead one to think that it will increase the precipitation over the whole globe, it does not occur homogeneously in all places. The reason for this is that precipitation is a complex process that depends on many factors (Drobinski et al. 2016), such as the presence of condensation nuclei in the atmosphere for cloud formation (Sato et al. 2018; Fanourgakis et al. 2019), horizontal advection of moisture (Llopart et al. 2020b), atmospheric instability etc. In a nutshell, it is

not expected that PRCTOT will increase concomitantly with air temperature increase.

P95 and R95p: The intensity of extreme daily rainfall events can be analysed by comparing the 95th percentile (P95) of the present and future climate. Since the percentile is a single value for the whole time slices, it is not possible to compute the hypothesis test to the mean differences. In DJF (Fig. 4e–h), all ensembles and scenarios show an increase in the intensity of the daily precipitation extremes over north-northeast Argentina and south of Brazil. Only GCMs show higher intensity of the daily precipitation extremes under RCP8.5 than RCP4.5 (Fig. 4g). Under RCP4.5, GCMs and Eta also project an increase of P95 in a large area of eastern Brazil. In this same region, but under RCP8.5, Eta shows a variable signal, indicating some areas with an increase and decrease of P95. In the SACZ region, Eta projects a decrease in the precipitation intensity (Fig. 4h). In JJA (Fig. 5e–h), all scenarios and ensembles indicate a decrease of P95 over northeast Argentina and northeast Brazil. Inversely, under the RCP4.5 scenario, the models project an increase in P95 over southern Brazil. Under the RCP8.5, this signal is reduced in area, reaching São Paulo State in GCMs and north-centre southern Brazil in Eta.

We identified the number of days in the future that exceeds the 95th percentile of the daily precipitation computed for the present climate conditions. This procedure was done to compare the frequency of extreme precipitation events in the future with the present climate. The same spatial configuration described to P95 is obtained to R95p and presents statistical significance. Then, attention may be addressed to southern Brazil since all scenarios, ensembles, and seasons indicate an increase in the frequency of extreme events (Figs. 4, 5i–l). Moreover, the band from Peru to Argentina along the Andes indicates a frequency increase of R95 in DJF. In JJA, this feature is projected only by GCMs. In general, our results agree with Chou et al. (2014b) and Blázquez and Solman (2020). These authors evaluated the climate change signal in an ensemble of GCMs and RCMs from the CORDEX project. It is worth mentioning that our results are also in agreement with the trends detected in the 1950–2018 period by Dunn et al. (2020). As Blázquez and Solman (2020), we highlight that R95p provides essential information for impact studies.

CDD and CWD: In order to facilitate the analysis of these two indices concomitantly, we present in brownish the increase in CDD (Figs. 4, 5 m–p) and the decrease in CWD (Figs. 4, 5q–t). In DJF, GCMs ensemble projects a significant statistical increase (decrease) in CDD (CWD) in almost the whole continent, with a more intense signal in RCP8.5. Eta ensemble differs from GCMs since it
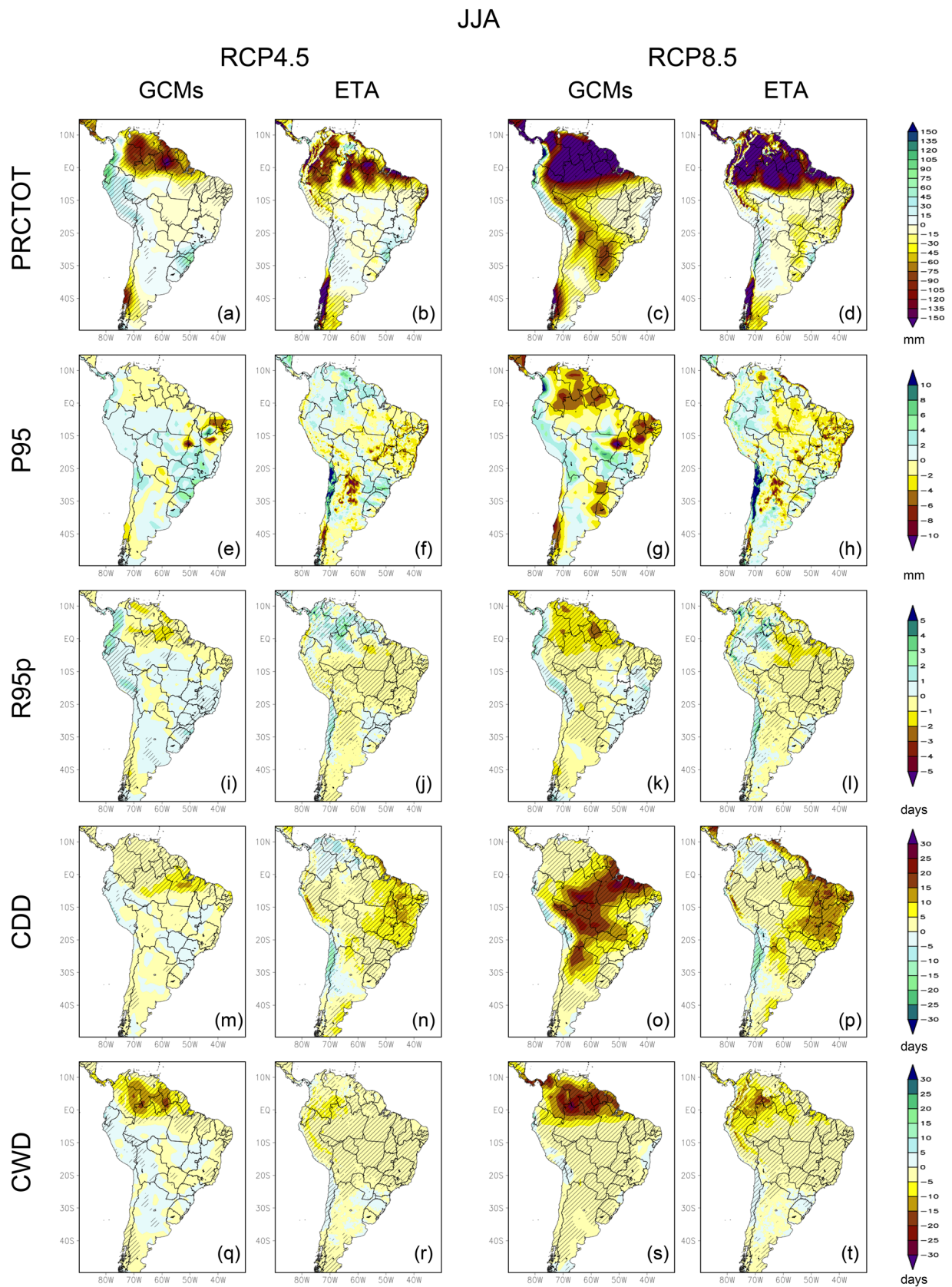
Fig. 5 Similar to Fig. 4 but for JJA

projects an increase of CDD over northern SA, the eastern coast of Brazil and Chile. In CWD, the decrease occurs in the SCAZ region and northern SA. It is worth mentioning that the Eta ensemble also indicates a decrease (increase) of CDD (CWD) over southeastern SA in both scenarios. In JJA, the ensembles again show differences in the spatial pattern of CDD and CWD. Concerning CDD, the highest increase occurs in a band over the north-northeast Brazilian regions in both ensembles and scenarios. In this season, the ensembles differ: while GCMs project an increase over centre SA, Eta projects the highest signal over northeast Brazil (Fig. 5m–p). The spatial signal projected by Eta is more similar to that obtained in the trends of the present climate in the CPC data (figure not shown). This result is also in agreement with that obtained in studies that use other datasets such as Ávila-Diaz et al. (2020). For CWD, there is again a significant decrease in this index over the continent. Its most intense signals are projected in both scenarios and ensembles over the extreme north of SA (Fig. 5q–t). Based on our results, the Amazon and northeast Brazil may be the sectors more affected by dry conditions in terms of CDD and CWD indices. These findings accord with those from studies for the present (Dereczynski et al. 2020; Dunn et al. 2020) and future climate (Chou et al. 2014a, b).

3.2.2 Minimum temperature

TN, TNn and TNx: Independently of scenario, season, index and ensemble, there is an increase statistically significant in the minimum temperature over the whole SA (Figs. 6, 7). In a general view, GCMs tend to be warmer (colder) than Eta to the north of (south of) 20°S. Considering TN, DJF and RCP8.5 (Fig. 6c, d), Eta projects an increase up to 5 °C between Argentina and Paraguay. In the GCMs, this increase is limited to 3 °C. Other RCMs also project in this same region maximum warming. For instance, in the framework of the CLARIS-LPB project, López-Franca et al. (2016), using four RCMs (LMDZ, RCA, PROMES, REMO) and A1B scenario, also found similar warming in TN.

TN10 and TN10p: TN10 is the 10th percentile computed for each time slice. In DJF (Fig. 6m–p), under RCP4.5, GCMs ensemble projects an increase of ~ 3 ℃ in almost all SA while Eta shows warmer conditions (~ 4 ℃) over southeastern SA. This configuration is also obtained in RCP8.5 but with Eta projecting an increase of TN10 higher 5 °C over southeastern SA. However, this signal is an austral summer feature. In JJA (Fig. 7m–p), Eta projects a decrease of 2 °C (1 °C) over southeastern SA and in a large area of Argentina under RCP4.5 (RCP8.5). On the other hand, in the same area, GCMs ensemble projects an increase in TN10 (2 °C for RCP4.5 and 3 °C for RCP8.5). GCMs ensemble also

projects warmer conditions (~ 1 °C) over the Amazon than Eta in both seasons and scenarios.

TN10p is also called cold nights and is the percentage of nights with minimum temperature below the 10th percentile computed from the present climate conditions. For all scenarios, seasons, and ensembles, there is a statistically significant decrease in the frequency of cold nights, mainly northern 20°S (Figs. 6–7q–t). This result partially agrees with López-Franca et al. (2016). In the CLARIS-LPB framework, although there is also a decrease in cold nights, the most significant change in the frequency occurs over southeastern Brazil. In DJF (Fig. 6q–t), both ensembles project a decrease higher than 9% in the frequency of cold nights to the north of 20°S under RCP4.5 and RCP8.5. Also, they project a decrease of ~ 6% in RCP4.5 and ~ 8% in RCP8.5 to the south of 20°S. The changes projected in JJA (Fig. 7q–t) are slightly lower than in DJF. For example, to the south of 20°S, the ensembles project a decrease of ~ 5% in RCP4.5 and ~ 7% in RCP8.5.

TN90 and TN90p: TN90 is the 90th percentile computed for each time slice from minimum temperature. TN90p is the percentage of days with a minimum temperature above the 90th percentile computed from the present climate conditions. The spatial pattern and changes projected to TN90 (Figs. 6–7u–x) are similar to those described in TN10 (Figs. 6–7 m–p). In DJF, the most remarkable change (5 °C) projected occurs over southeast SA by Eta and over extreme north of SA by GCMs, both under RCP8.5. In JJA, the GCMs ensemble projects an increase in TN90 on the whole continent. Inversely, Eta shows a decrease of this variable over southeastern SA in ~ 1 °C under RCP4.5 and practically no decrease under RCP8.5.

TN90p is also called warm nights (Figs. 6–7y–ab). This index shows positive and more prominent changes than TN10p, which has a negative signal in the order of 10%. While TN10p is becoming less frequent, TN90p is acquiring a higher frequency, being an indicator of the warming climate in the future. These results follow those obtained by López-Franca et al. (2016) under the A1B scenario. In DJF (Fig. 6y–ab), the GCMs ensemble projects a higher percentage of TN90p compared to the Eta ensemble. For instance, over the southern Amazon, there is a percentage of 70% (40%) simulated by GCMs (Eta) under RCP4.5. Over southeastern SA, there is a gradient in the percentage, which decreases to the south of 25°S. Considering RCP8.5, TN90p reaches 90% over the southern Amazon in the GCMs projections and 65% over northwest SA and north of northeast Brazil in the Eta projections. For JJA (Fig. 7y–ab), the most remarkable changes appear over the extreme north of SA, reaching 90% in both ensembles under RCP8.5. In GCMs, these changes cover a large area. On the other hand, over southeastern SA, the Eta ensemble projects more significant

Fig. 6 Changes (future minus present) projected to the minimum temperature climate indices from GCMs and Eta ensembles in DJF: **a–d** TN (°C), **e–h** TNn (°C), **i–l** TNx (°C), **m–p** TN10 (°C), **q–t** TN10p (%), **u–x** TN90 (°C) and **y–ab** TN90p (%). From left to right: GCMs and Eta ensembles under RCP4.5 and RCP8.5, respectively. Cross-hatching presents differences statistically significant at 0.1 confidence level
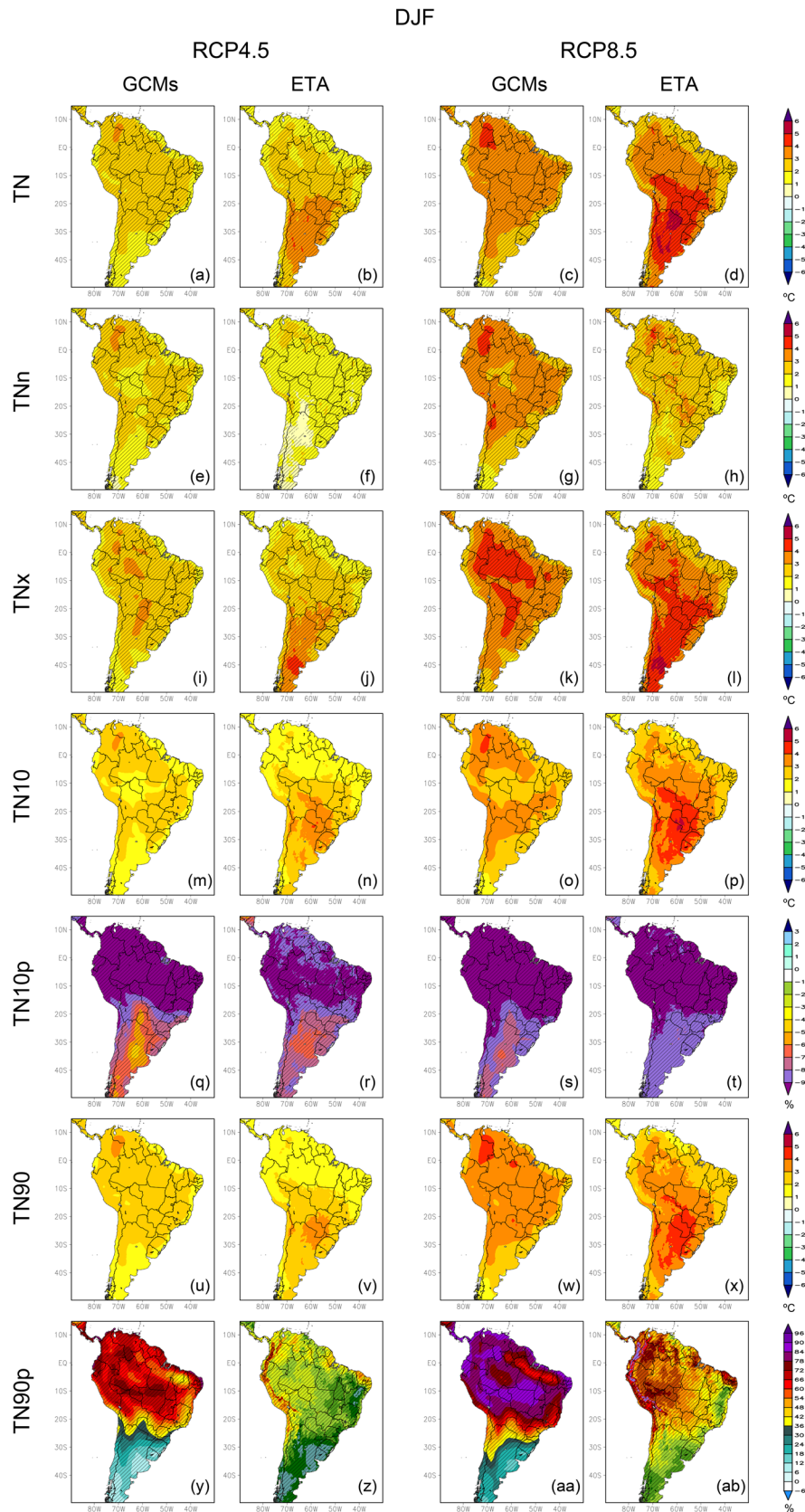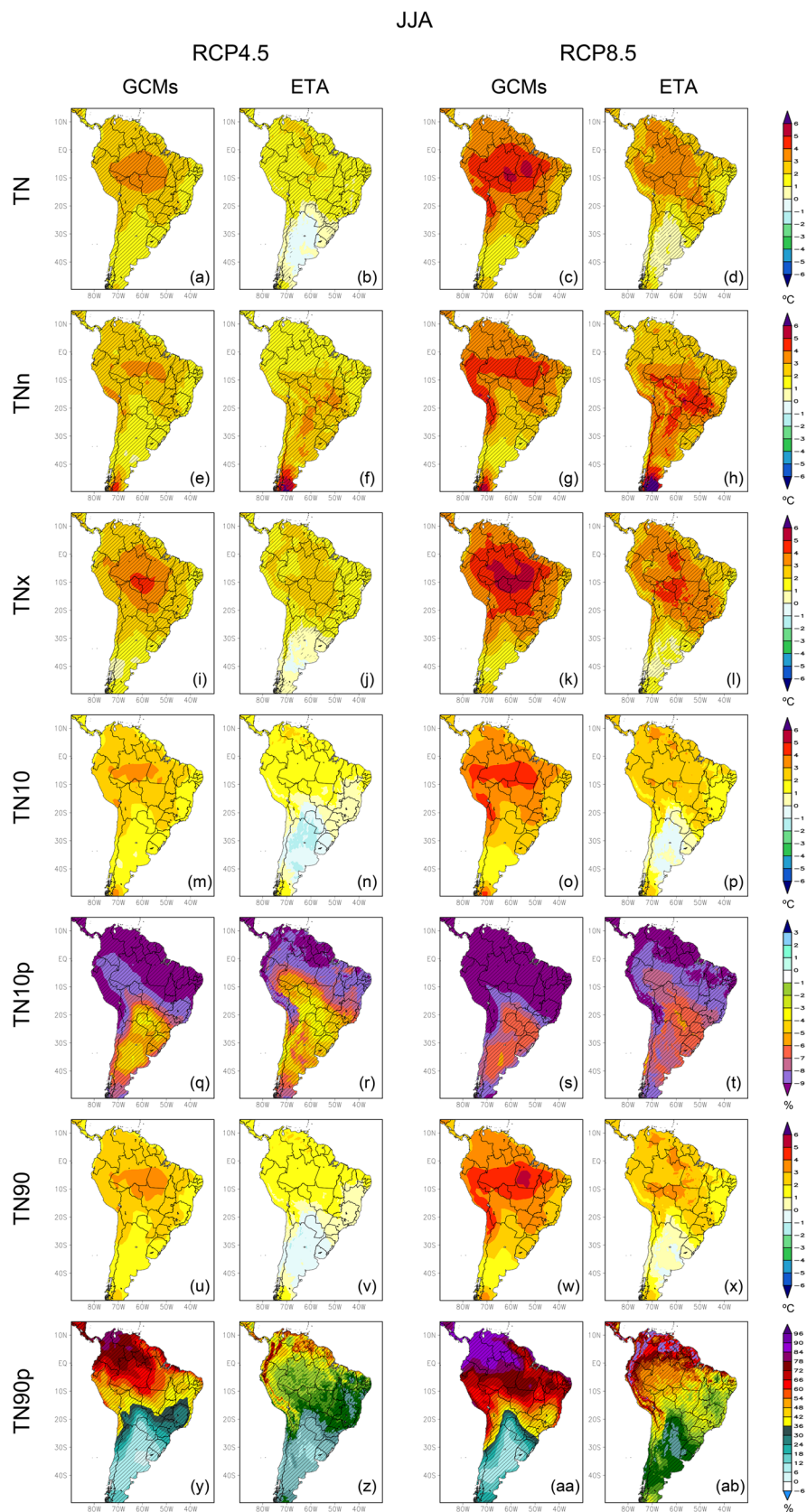
Fig. 7 Similar to Fig. 6 but for JJA

changes than GCMs. The percentages projected under RCP8.5 agree with those obtained under the A1B scenario by López-Franca et al. (2016).

3.2.3 Maximum temperature

TX, TXn and TXx: As well as for the minimum temperature, independently of scenario, season and ensemble, the maximum temperature indices show an increase statistically significant over the whole SA (Figs. 8, 9). Exceptions to this occur in southeastern SA during JJA in Eta projections (Fig. 9b, f, j, n, r, v for RCP4.5 and Fig. 9d, l, p, x for RCP8.5). In DJF, under RCP4.5, the warming is higher in the central part of Brazil (4–5 °C) in both ensembles. Under RCP8.5, the Eta ensemble shows two cores of higher warming: one over the Amazon and another between centre-west and southeast Brazil with ~ 6 °C (Fig. 8d, h, l). The spatial patterns of the RCP4.5 scenario projections are more similar to those of López-Franca et al. (2016) for scenario A1B. In JJA, the indices (TX, TXn, and TXx) are higher over the southern Amazon. For both scenarios, GCMs ensemble projects the higher temperatures (Fig. 9a–j). Conversely, Eta projects under RCP4.5 a negative temperature trend ranging from − 2 to − 3 °C that is up to 1 °C under RCP8.5.

TX10 and TX10p: TX10 is the 10th percentile computed for each time slice from maximum temperature. TX10p is the percentage of days with a maximum temperature below the 10th percentile computed from the present climate conditions. TX10p is also called cold days. From Figs. 8 and 9 m–p, it is clear that Eta projects higher values of TX10 in DJF and GCMs in JJA. The highest values of TX10 are projected under RCP8.5. For example, in DJF, the changes projected by Eta are 2 ℃ over the north of northeast Brazil and the western boundary of SA. In a large part of the continent between 25°S and 10°N, Eta projected changes are up to 5 ℃.

Considering TX10p, it is negative and statistically significant over the whole continent in DJF (Fig. 8q–t). These results indicate that the number of cold days is projected to decrease in the future climate. This decrease is pronounced in the GCMs ensemble to the north of 20°S (> 9%) in both scenarios. In the Eta ensemble, it is more concentrated in the SACZ region (7–8%). In JJA (Fig. 9q–t), the decrease in the frequency of cold days is still higher to the north of 20°S compared with DJF. Nevertheless, to the south of 20°S, it has a slight decrease with the Eta ensemble showing no changes from southern Bolivia to the centre of Argentina under RCP4.5. The changes projected in TX10p in both scenarios have a similar magnitude and spatial distribution to those under scenario A1B (López-Franca et al. 2016). In terms of spatial pattern, these changes occur in the same

place where there is an increase in this variable from 1950 ahead (Dunn et al. 2020; Dereczynski et al. 2020).

TX90 and TX90p: TX90 is the 90th percentile computed for each time slice from maximum temperature. TX90p, also called warm days, is the percentage of days with a maximum temperature above the 90th percentile computed from the present climate conditions. The changes projected to TX90 are similar to those of TX10 in terms of spatial pattern and magnitude. Nonetheless, it does not occur to TX90p and TX10p since TX90p has a very high increase (in module) than TX10p. It means that the increase in the frequency of warm days is higher than that of the decrease of cold days. In DJF (Fig. 8y–ab), regions like the Amazon, north of SA and north of northeast Brazil, show the highest increase in TX90p, higher 65% in both ensembles under RCP8.5. In JJA (Fig. 9y–ab), in both scenarios and ensembles, the changes are more remarkable to the north of 20°S and lower to the south of this latitude when compared with DJF. Again, the Amazon and north of northeast of Brazil present the most notable changes, greater than 70% under RCP8.5.

In summary, for the temperature, ensembles project warmer conditions under RCP8.5 over the whole continent. Projections characterize the cold nights and days' frequency decrease (TN10p and TX10p) and the warm nights and days' frequency increase (TN90p and TX90p). Moreover, the percentage of change is higher for warm nights and days compared to cold ones. Another interesting result is that in the tropical region (to the north of 20°S), the warm nights' percentage change overtakes that of warm days.

Although we have not explored other variables (such as long and short wave radiation and cloud cover) to explain how warm nights increase more than warm days, some hypotheses are based on the literature (Dai et al. 1999; Zhou et al. 2009; López-Franca et al. 2016). Considering (a) that the capacity of the air to maintain water vapour in a warmer climate is higher than in the historical period (that follows the equation of Clausis-Cleyperon), (b) that water vapour is the main greenhouse gas and (c) a great concentration of other greenhouse gases in the atmosphere, it is assumed that there is less loss of longwave radiation from the surface to space at night. Greenhouse gases keep the energy captured at the surface during the day, warming the surface at night, leading to a warmer minimum temperature. On the other hand, greenhouse gases are not able to absorb shortwave radiation emitted by the Sun. Then, during the daytime, this energy reaches the surface. However, not all the energy emitted by the Sun reaches the surface because of the albedo effect of clouds. Dai et al. (1999) and López-Franca et al. (2016) mention that the influence of clouds has opposite effects

Fig. 8 Changes (future minus present) projected to the maximum temperature climate indices from GCMs and Eta ensembles in DJF: **a–d** TX (°C), **e–h** TXn (°C), **i–l** TXx (°C), **m–p** TX10 (°C), **q–t** TX10p (%), **u–x** TX90 (°C) and **y–ab** TX90p (%). From left to right: GCMs and Eta ensembles under RCP4.5 and RCP8.5, respectively. Cross-hatching presents differences statistically significant at 0.1 confidence level
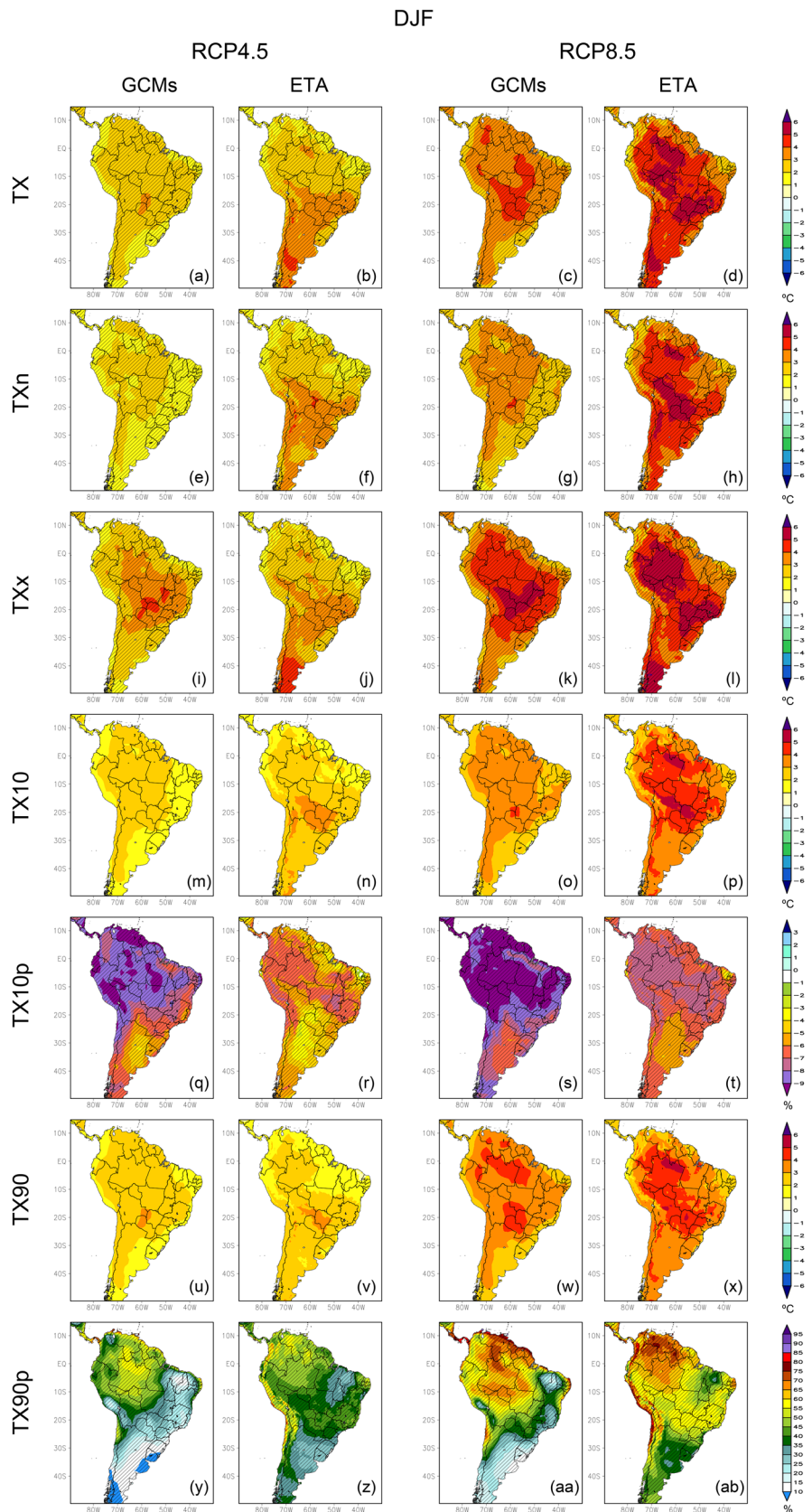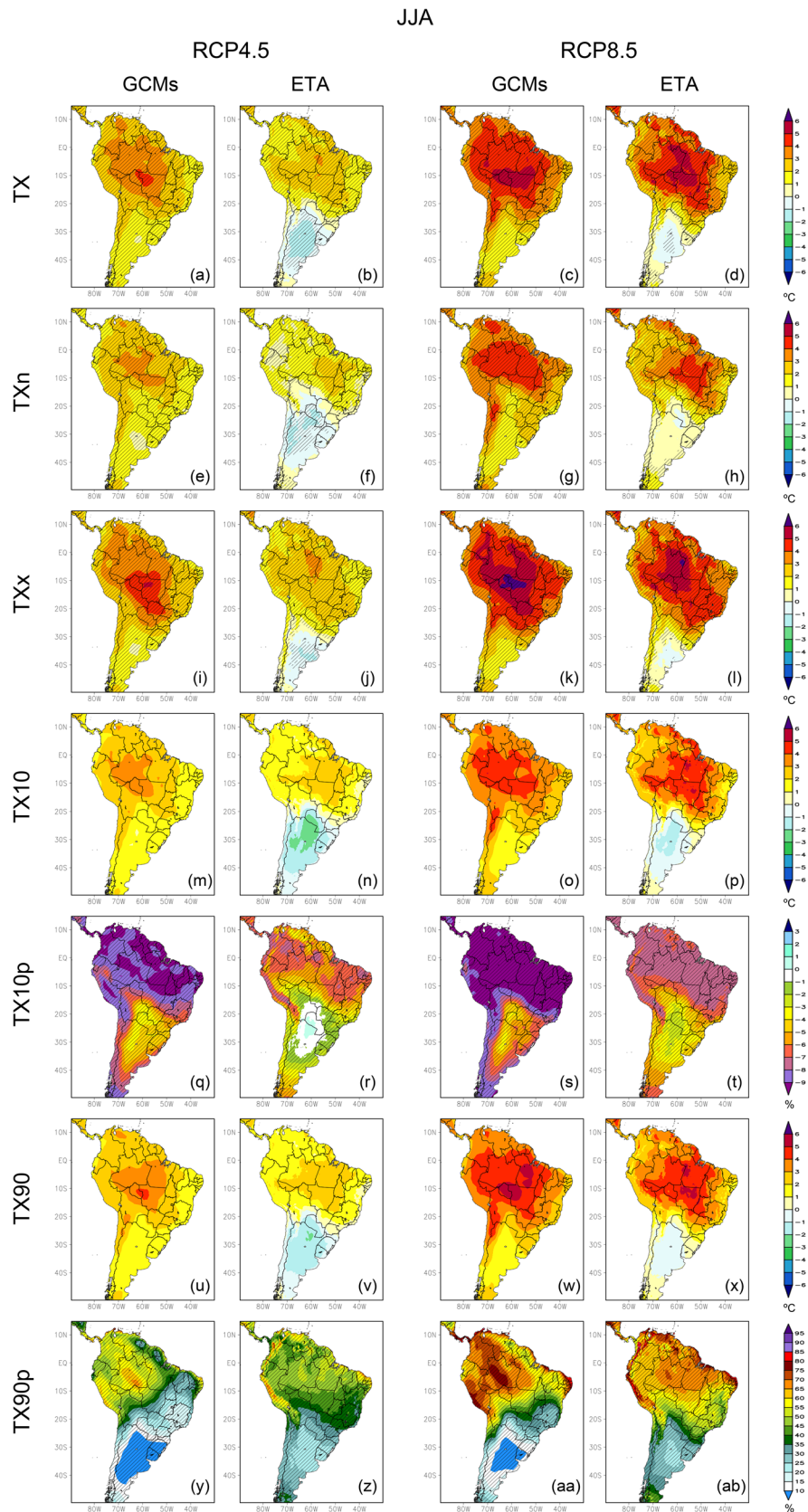
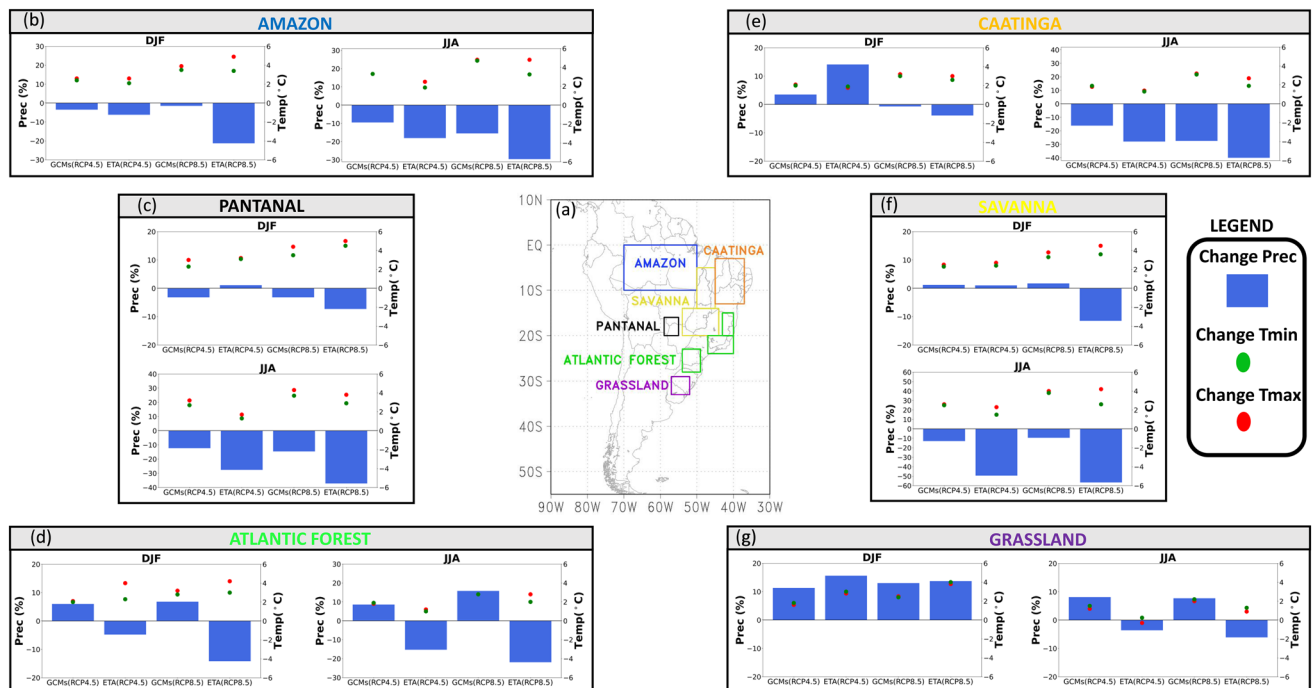**Fig. 9** Similar to Fig. 8 but for JJA

Fig. 10 Changes projected over six SA biomes by GCMs and Eta ensembles for DJF and JJA precipitation (bars), minimum temperature (green line) and maximum temperature (red line) under RCP4.5 and RCP8.5 in the 2050–2080 period

on night and day processes. According to these authors, clouds can reduce the maximum temperature by reflecting the shortwave radiation and increase the minimum temperature by enhancing downward longwave radiation. Then, the clouds may contribute to a higher percentage of warm nights than warm days in the future climate. We also highlighted that although Sect. 3.2.1 shows a decrease in PRCTOT and CWD, it does not mean that the cloud cover will decrease in the future climate. This hypothesis is supported by Zhou et al. (2009) projections that show a slight change in the shortwave radiation (~ -6 W m^2) and changes reaching ~ 30 W m^2 in the longwave radiation.

3.3 Summary of the projected changes focusing on Brazil

Previous sections showed that the signal of the climate changes projected over SA has different spatial and temporal variability. In order to summarise the results focusing on Brazil (which covers 48% of the SA area, Worldometer 2021), Fig. 10 shows, for each Brazilian biome, the percentage changes in the precipitation and the average changes of minimum (TN) and maximum temperature (TX) under RCP4.5 and RCP8.5. The country was divided into biomes instead of administrative regions due to two reasons: (a) follow the analyses of the Climate Change Brazilian Panel (PBMC 2013, 2020) and Almagro et al. (2020) and (b) because the biomes have proper environmental features (i.e.,

climate, vegetation etc.), which is not the case when the country is divided by administrative regions. A numerical modelling study of the climate change impacts on the vegetation/species is beyond the scope of this study (for example, to analyse the vegetation changes, models of dynamic vegetation are necessary; Potter 2004; Cubasch et al. 2013). However, we include a brief review of the literature on this subject for each Brazilian biome. Moreover, some pieces of information on the impacts of climate change on water availability and agriculture is included in this section.

Amazon forest: dry conditions and higher temperatures characterize the climate changes in this biome. Precipitation is projected to decrease in all ensembles, seasons and scenarios. Eta ensemble under RCP8.5 indicates a precipitation decrease of 20% in DJF and $\sim 30\%$ in JJA. TX shows a higher increase compared to TN. For example, the Eta ensemble projects an increase of ~ 5 °C in DJF and JJA under RCP8.5 (Fig. 10b). Concerning the species distribution, the dry and warmer conditions in the Amazon Forest can lead to a savannization of this region (Stark et al. 2020). According to Marengo et al. (2011), savannization is expected if the warming is above 3.5–4 °C due to increased greenhouse gases concentrations. Lyra et al. (2016) used a dynamic vegetation model forced by the Eta model driven by HadGEM2-ES. In the Amazonian region, the authors obtained that some rainforest areas may be replaced by deciduous forest type and grassland under RCP4.5 and only by grassland under

RCP8.5 scenario at the end of this century. Under RCP4.5 (RCP8.5) is projected a reduction of ~9% (50%) in the area of tropical forest. Marengo et al. (2018a) highlight that the land-use change in the future depends on socio-economic factors defined in the IPCC scenarios. These same authors also present a review of climate change impacts on the Amazon region. We mentioned some studies that evaluate the impact of atmospheric warming on the species. However, other studies simulate the impact of deforestation on the climate (e.g. Llopart et al. 2018). Concerning the current climate, the Amazon region has recorded periods of droughts. From 2005, Amazon experienced three severe droughts caused by different drivers (Zou et al. 2016; Jimenez et al. 2018). Observational studies also have shown a substantial reduction in the leaf area index (LAI) as forest loss increased (Baker and Spracklen 2019), with evapotranspiration (ET) showing a decline (Baker and Spracklen 2019; Oliveira et al. 2021). These variations are related to changes in temperature, with increased warming as deforestation increased (Baker and Spracklen 2019).

Pantanal: Precipitation decrease is the dominant signal in this region, mainly in JJA, reaching ~40% in the Eta ensemble under RCP8.5. For the temperatures, the most substantial changes are projected to DJF (4–5 °C) under RCP8.5 (Fig. 10c). Pantanal is the world's largest freshwater wetland (Schulz et al. 2019; Lázaro et al. 2020). Therefore, the future deficit of precipitation in this biome may cause a tremendous negative impact on the species that depend on water availability. Colman et al. (2019) analysed the impact of climate change on land use in Pantanal. They computed the average annual soil erosion for the baseline (2012) and projected scenarios for 2020, 2035, and 2050. For the worst scenario, the cropland expansion in some parts of the highlands may increase the soil loss up to 100% (2012–2050). For the same period, it is projected an increase of 20–40% in soil loss in parts of the Pantanal biome, associated with farmland increase (mainly for livestock) in the lowlands. Alho et al. (2019) describe the threats to the Pantanal biodiversity due to land use and occupation. In this observational study, the authors mention that the influence of the flood variability in annual and inter-annual scales can be evidenced in the field through specific vegetation patterns. According to this study, two trends are observed: (a) in prolonged drought events, some woody plants colonize the former seasonally flooded fields with homogeneous formations, and (b) in prolonged periods of flood, water-tolerant trees are observed to form homogeneous or monodominant blocks. A case of prolonged drought in Pantanal has been registered since 2019, with subsequent fires engulfing hundreds of thousands of hectares (Marengo et al. 2021). In 2020, the river levels reached shallow values, and transportation had to be restricted in some parts of the rivers (Marengo et al. 2021). According to Leal

Filho (2021), the area affected by fires in 2020 (around 3.9 million hectares) is more than twice the area burnt in 2019 and corresponds approximately to the combined areas of Rio de Janeiro and São Paulo cities. Lázaro et al. (2020) also found that Northern Pantanal has 13% more days without rain than in the 1960s, and the water mass is 16% less during the dry season considering the last ten years. It is an indication that the Pantanal is losing water and experiencing a more severe drought season than in the past.

Atlantic forest: In this biome, the ensembles are discordant in terms of the climate change signal for precipitation. While GCMs ensemble projects an increase in precipitation in both seasons and scenarios, the Eta ensemble projects a decrease. The changes in the temperature range from 2 to 4 °C (Fig. 10d). As more than 60% of the Brazilian people live within the Atlantic Forest domain, climate changes in this biome can cause significant social vulnerability (Scarano and Ceotto 2015). Regarding the distribution of species, changes in precipitation and increased temperature can lead to the animals' extinction since habitat becomes inadequate for the species (Loyola et al. 2014; Scarano and Ceotto 2015; Moraes et al. 2019). For example, Lima et al. (2019) investigated how climate changes scenarios will influence primate biodiversity. They found that regions closer to Savanna will face a reduction in primate richness. It is also projected community heterogenization driven by the reduction of species geographic distributions, and the most remarkable temporal changes are projected for the midwest and central region of the Atlantic Forest biome. Moraes et al. (2019) evaluated the effects of climate change on climatically suitable areas for the occurrence of snakes, considering the responses of distinct reproductive groups (oviparous and viviparous). Their projections indicate that 73.6% of oviparous species and 67.6% of viviparous species could lose at least half of their original range by 2080. Atlantic Forest is projected to warm in the future scenarios and, consequently, acquire adequate conditions for the sylvatic mosquito (primary vector of *Plasmodium* spp.), which can cause malaria in humans outside the Amazon biome (Azevedo et al. 2019).

Semi-arid or Caatinga (Brazilian name): In DJF under RCP4.5, the ensembles project an increase in precipitation, and under RCP8.5, a slight decrease of this variable. Inversely, in JJA, the ensembles under both scenarios project a decrease of precipitation that reaches 25% (40%) in the Eta ensemble under RCP4.5 (RCP8.5). The different climate change signals in DJF scenarios can be associated with the internal variability of the climate system to the different levels of warming (Deser et al. 2012). This kind of signal does not occur only over SA. For instance, Ali et al. (2020) showed opposite signals in the precipitation projected for Pakistan under RCP4.5 and RCP8.5. The

changes in temperature in Caatinga ranges between 2 and 3 °C (Fig. 10e). Caatinga is a biome located in the second drier region in South America (Reboita et al. 2010) and can be considered a "semi-arid island" inside tropical latitudes. The most important driver for this semi-arid climate is the subsidence branch of the intense convection in the Amazon Forest (Reboita et al. 2016). The drier conditions projected for Caatinga can increase the aridity and, consequently, desertification processes, loss in local biodiversity (Oliveira et al. 2012; PBMC 2013; Vieira et al. 2015; Rodrigues et al. 2015) and increasing food insecurity (Lemos et al. 2016). Oliveira et al. (2012), through two greenhouse gas emission scenarios for 2020, 2050, and 2080, suggest that natural vegetation remnants will likely play a role as climate refuges for the Caatinga biome's endemic vertebrate species. Souza e Silva et al. (2019) also mention that plant species endemic to the Caatinga are highly vulnerable to even conservative scenarios of future climate change and may lose much of their climatic envelopes. During the last years, Caatinga registered the longest sequence of dry years (2010–2017) with a consequent reduction in water availability and a direct effect on the mortality and recruitment of woody species as well as shrubby-tree individuals of smaller diameter showing less resilience to the cumulative effect of drought (Marengo et al. 2018b; Campos et al. 2020). In addition, these severe drought conditions have in recent years caused a decrease in the volume of hydroelectric reservoirs, such as Sobradinho and Itaparica (Cunha et al. 2019; Vasquez-Arroyo et al. 2020).

Savanna or Cerrado (Brazilian name): For DJF, the only significant change projected to the precipitation is by the Eta ensemble under RCP8.5 (~ 10%). Nonetheless, for JJA, in both scenarios, GCMs ensemble projects a deficit of ~ 10% while Eta ensemble projects more than 50% (Fig. 10f). Since JJA is the dry season in the Savanna biome, a future precipitation decrease may significantly impact the water supply and other activities in this region. The projected increase of temperature in this region is ~ 3 °C (~ 4 °C) in RCP4.5 (RCP8.5). These simultaneous changes in decreasing precipitation and increasing temperature may compromise agriculture (Zilli et al. 2020) and hydropower generation (Oliveira et al. 2019; Rodrigues et al. 2020). Under RCP4.5 and RCP8.5, Zilli et al. (2020) obtained with GBLOBIOM-Brazil by 2050 a decrease in soybeans and corn production, mainly in the Northern Cerrado, and southward displacement of agricultural production to near-subtropical and subtropical regions of the Cerrado and the Atlantic Forest biomes. Caetano et al. (2018), for the period 2080–2100 under RCP4.5, project a decrease in soybean production by up 50% in the central region of Brazil. For coffee production, Zullo Junior et al. (2006, 2008) simulated three scenarios: temperature increasing in 1 °C, 3 °C and 5.8 °C concomitant

with a 15% increase in precipitation. For São Paulo state, in the more pessimistic scenario, the area suitable for this production decreases for 3.3% compared to the present climate. Another problem in the Savanna biome is the fires, mainly during the dry season (Silva et al. 2019b) and the beginning of spring (Santos et al. 2019), which negatively impact biodiversity. Concerning the Savanna biodiversity, Borges and Loyola (2020) identified the refugia areas for bird species considering projections for 2050 under the RCP8.5 scenario. Results indicate that regions with more native vegetation in the north and northeast Savanna may be further vulnerable to higher values of temperature and precipitation anomalies. While 35.4% of the biome are high-risk areas exposed to high climate anomalies and poor native vegetation, only 13% of the territory may be potential refugia for bird species since those areas are more likely to retain native vegetation and face low climatic anomalies. Savanna has experienced climate extremes in the last decade with the severe drought in the 2014 and 2015 summers (Reboita et al. 2015; Coelho et al. 2016), which led to the major hydric crises and a decrease in the volume of hydroelectric reservoirs, such as Cantareira and Três Marias (Nobre et al. 2016; Cunha et al. 2019; Vasquez-Arroyo et al. 2020).

Grassland: In DJF, both ensembles and scenarios agree with the precipitation increase being higher than 10%. In JJA, GCMs ensemble projects an increase of precipitation in both scenarios, while Eta ensemble projects a decrease. For the temperatures in DJF, the projected changes reach 4 °C, while in JJA, it is lower than 2 °C (Fig. 10g). Concerning biodiversity, these conditions can lead to the extinction of species or changes in plants distribution patterns of this biome (Giudicelli et al. 2019; Trindade et al. 2020). For soybeans, while it is projected to decrease production in the Savanna biome by 2080–2100, Grassland will have more favourable conditions, with an increase of ca. 25% (Caetano et al. 2018). Streck et al. (2012) observed the changes in agriculture in the last decades (from 1912 to 2011) and mentioned that temperature increase was responsible for changing the rice phenology. Over the studied period, rice culture showed anticipation of harvest time of 17–31 days, which is related to trends of temperature increase during the growing season.

From the previous discussion, it is clear that climate change causes alterations in the phenology and composition of ecological communities (Parmesan 2006; Chen et al. 2011). Moreover, tropical species are more vulnerable to climate changes since they live near their maximum thermal tolerance, have high sensibility and low adaptation capacity (Araújo et al. 2013; Foden et al. 2013; Khaliq et al. 2014; Borges and Loyola 2020). Hence, these outcomes provide important information for the ecological/environmental areas seeing that climate changes cause variations in species distribution (Walther et al. 2002). Climate change effects

on forest biodiversity and ecosystem functions are associated with changes in forest structural complexity (Stark et al. 2012; Stein et al. 2014; Gough et al. 2019; Penone et al. 2019; Ehbrecht et al. 2021). Therefore, assessing the impacts of climate change on different tropical forests demands a profound understanding of how climate controls and shapes forest compositional and functional diversity (Kreft and Jetz 2007; Harrison et al. 2020; Ehbrecht et al. 2021). To finish this section, as Titeux et al. (2016), we suggest that studies that evaluate the impacts of environmental changes on biodiversity should not only focus on climate changes but also on land-use changes.

4 Conclusions

The skill of two ensembles (GCMs and Eta) in reproducing SA climate is presented here. These ensembles were based on daily precipitation and minimum and maximum temperatures for the 1980–2015 period. Besides, changes projected by the ensembles under the RCP4.5 and RCP8.5 scenarios for the 2050–2080 period were also performed.

Validation: Both GCMs and Eta ensembles capture spatial and temporal variability of precipitation and mean temperature over SA. This good representation is also observed in terms of climate indices but with differences in intensity. For example, P95, an indicator of the daily rainfall extreme intensity, is less intense over southeastern SA in both ensembles and seasons. In DJF, this feature may indicate that the models cannot simulate the mesoscale convective systems that are a climatological characteristic of that region (Salio et al. 2007; Demaria et al. 2011). Eta shows some improvements in simulating the SA present climate compared to GCMs. For instance, Eta corrects the precipitation overestimation over the Andes in DJF and simulates the observed values of maximum precipitation over southern Brazil in JJA. For these reasons, we can consider that Eta adds value to GCMs. In terms of trends, precipitation ensembles (Eta and GCMs) do not compare well with observations, while temperature trends have more similarities with CPC.

Future climate: Southeastern SA, Amazon and northeast Brazil are the regions more vulnerable to climate changes. In southeastern SA, it is due to the impacts of higher frequency and intensity of daily rainfall extremes and increase of CWD. In the Amazon, the projections indicate drier conditions compared to the historical period. Lastly, northeast Brazil appears vulnerable in JJA when the models project an increase (decrease) of CDD (CWD). Furthermore, over the whole SA, is projected to have an increase in the temperature being higher under RCP8.5. The results also indicate a

decrease (increase) in the frequency of cold (warm) nights and days. Additionally, the percentage of change is higher for warm nights and days compared to cold ones. In the tropical region (to the north of 20°S), the warm nights' change overtakes that of warm days. Considering the Brazilian biomes in DJF and JJA, they may be affected by an increased temperature, while precipitation is more variable across the ecosystems. For example, in the Amazon Forest is projected a decrease of more than 10% in seasonal precipitation amounts, while in Grassland (south of Brazil) is expected an increase of more than 10% compared to the present climate.

Support for policymakers' decision: This study is a source of helpful information for policymakers since they need to prepare strategies for several impacts of climate change. These impacts may lead to effects such as (a) on public health due to the thermal stress caused by the occurrence of persistent warm temperatures and increase of diseases like malaria; (b) demand of energy and water availability due to high temperatures projected for the future; (c) natural disasters associated with heavy rainfall events mainly in poor communities.

Final message: Climate models are tools used to represent the climate, and when applied to the future, they include suppositions of human activities (scenarios). Thus, climate projections involve uncertainties that are associated with different sources (Hawkins and Sutton 2009; Giorgi 2010; Latif 2011; Gettelman and Rood 2016): model uncertainty (model design and physical parameterization schemes); initial and boundary conditions; scenario uncertainty; and internal variability of the climate system. Therefore, the results obtained in the projections are not the absolute truth of climate in the future. Instead of that, they are indicative of the future assuming certain lifestyles. In this way, the projections are the best information source for the policymakers developing their strategies and actions of mitigation and sustainability.

References

Alexander LV, Zhang X, Peterson TC et al (2006) Global observed changes in daily climate extremes of temperature and precipitation. J Geophys Res Atmos 111:D05109. https://doi.org/10.1029/2005JD006290

Alexander LV, Fowler HJ, Bador M et al (2019) On the use of indices to study extreme precipitation on sub-daily and daily time scales. Environ Res Lett 14:125008. https://doi.org/10.1088/1748-9326/ab51b6

Alho CJ, Mamede SB, Benites M, Andrade BS, Sepúlveda JJ (2019) Threats to the biodiversity of the Brazilian Pantanal due to land use and occupation. Ambiente Soc. https://doi.org/10.1590/1809-4422asoc201701891vu2019L3AO

Ali S, Kiani RS, Reboita MS et al (2020) Identifying hotspots cities vulnerable to climate change in Pakistan under CMIP5 climate projections. Int J Climatol. https://doi.org/10.1002/joc.6638

Almagro A, Oliveira PTS, Rosolem R et al (2020) Performance evaluation of Eta/HadGEM2-ES and Eta/MIROC5 precipitation simulations over Brazil. Atmos Res 244:105053. https://doi.org/10.1016/j.atmosres.2020.105053

Ambrizzi T, Reboita MS, Rocha RP, Llopart M (2019) The state of the art and fundamental aspects of regional climate modeling in South America. Ann N Y Acad Sci 1436:98–120. https://doi.org/10.1111/nyas.13932

Araújo MB, Ferri-Yáñez F, Bozinovic F et al (2013) Heat freezes niche evolution. Ecol Lett 16:1206–1219. https://doi.org/10.1111/ele.12155

Arora VK, Scinocca JF, Boer JG et al (2011) Carbon emission limits required to satisfy future representative concentration pathways of greenhouse gases. Geophys Res Lett 38:L05805. https://doi.org/10.1029/2010GL046270

Ashfaq M, Cavazos T, Reboita MS et al (2020) Robust late twenty-first century shift in the regional monsoons in RegCMCORDEX simulations. Clim Dyn. https://doi.org/10.1007/s00382-020-05306-2

Ávila-Diaz A, Benezoli V, Justino F et al (2020) Assessing current and future trends of climate extremes across Brazil based on reanalyses and earth system model projections. Clim Dyn 55:1403–1426. https://doi.org/10.1007/s00382-020-05333-z

Azevedo TS, Lorenz C, Chiaravalloti-Neto F et al (2019) *Kertszia cruzii* and extra-Amazonian malaria in Brazil: challenges due to climate change in the Atlantic Forest. Infect Genet Evol 85:104456. https://doi.org/10.1016/j.meegid.2020.104456

Baker JC, Spracklen DV (2019) Climate benefits of intact Amazon forests and the biophysical consequences of disturbance. Front for Glob Change 2:47. https://doi.org/10.3389/ffgc.2019.00047

Beniston M, Stephenson DB (2004) Extreme climatic events and their evolution under changing climatic conditions. Glob Planet Change 44:1–9. https://doi.org/10.1016/j.gloplacha.2004.06.001

Blázquez J, Solman SA (2019) Relationship between projected changes in precipitation and fronts in the austral winter of the Southern Hemisphere from a suite of CMIP5 models. Clim Dyn 52:5849–5860. https://doi.org/10.1007/s00382-018-4482-y

Blázquez J, Solman SA (2020) Multiscale precipitation variability and extremes over South America: analysis of future changes from a set of CORDEX regional climate model simulations. Clim Dyn 55:2089–2106. https://doi.org/10.1007/s00382-020-05370-8

Borges FJA, Loyola R (2020) Climate and land-use change refugia for Brazilian Cerrado birds. Perspect Ecol Conserv 18:109–115. https://doi.org/10.1016/j.pecon.2020.04.002

Boroneant C, Plaut G, Giorgi F, Bi X (2006) Extreme precipitation over the Maritime Alps and associated weather regimes simulated by a regional climate model: present-day and future climate scenarios. Theoret Appl Climatol 86:81–99. https://doi.org/10.1007/s00704-005-0211-7

Caetano JM, Tessarolo G, Oliveira G et al (2018) Geographical patterns in climate and agricultural technology drive soybean productivity in Brazil. PLoS ONE 13:e0191273. https://doi.org/10.1371/journal.pone.0191273

Calheiros DF, Oliveira MD, Padovani CR (2012) Hydro-ecological processes and anthropogenic impacts on the ecosystem services of the Pantanal wetland. In: Ioris AAR (ed) Tropical wetland management: the south-American Pantanal and the international experience. Ashgate Publishing, Farnham, pp 29–57

Campos DA, Andrade EM, Castanho AD et al (2020) Biomass dynamics in a fragment of Brazilian Tropical Forest (Caatinga) over consecutive dry years. Appl Sci 10:7813. https://doi.org/10.3390/app10217813

Carvalho LMV, Jones C, Liebmann B (2004) The South Atlantic Convergence Zone: intensity, form, persistence, and relationships with intraseasonal and interannual activity and extreme rainfall. J Clim 17:88–108. https://doi.org/10.1175/1520-0442

Céron WL, Kayano MT, Andreoli RV et al (2020) Recent intensification of extreme precipitation events in the La Plata Basin in Southern South America (1981–2018). Atmos Res 249:105299. https://doi.org/10.1016/j.atmosres.2020.105299

Chen CT, Knutson T (2008) On the verification and comparison of extreme rainfall indices from climate models. J Clim 21:1605–1621. https://doi.org/10.1175/2007JCLI1494.1

Chen M, Shi W, Pingping X et al (2008) Assessing objective techniques for gauge-based analyses of global daily precipitation. J Geophys Res 113:D04110. https://doi.org/10.1029/2007JD009132

Chen I, Hill JK, Ohlemüller R et al (2011) Rapid range shifts of species associated with high levels of climate warming. Science 33:1024–1026. https://doi.org/10.1126/science.1206432

Chou SC, Marengo JA, Lyra AA et al (2012) Downscaling of South America present climate driven by 4-member HadCM3 runs. Clim Dyn 38:635–653. https://doi.org/10.1007/s00382-011-1002-8

Chou SC, Lyra A, Mourão C et al (2014a) Evaluation of the Eta simulations nested in three global climate models. Am J Clim Change 3:438–454. https://doi.org/10.4236/ajcc.2014.35039

Chou SC, Lyra A, Mourão C et al (2014b) Assessment of climate change over South America under RCP 4.5 and 8.5 downscaling scenarios. Am J Clim Change 3:512–527. https://doi.org/10.4236/ajcc.2014.35043

Chylek P, Li J, Dubey MK et al (2011) Observed and model simulated 20th century Arctic temperature variability: Canadian Earth System Model CanESM2. Atmos Chem Phys 11:22893–22907. https://doi.org/10.5194/acpd-11-22893-2011

Coelho CAS, Oliveira CP, Ambrizzi T et al (2016) The 2014 southeast Brazil austral summer drought: regional scale mechanisms and teleconnections. Clim Dyn 46:3737–3752. https://doi.org/10.1007/s00382-015-2800-1

Collins WJ, Bellouin N, Doutriaux-Boucher M et al (2011) Development and evaluation of an Earth-System model—HadGEM2. Geosci Model Dev 4:1051–1075. https://doi.org/10.5194/gmd-4-1051-2011

Colman CB, Oliveira PTS, Almagro A, Soares-Filho BS, Rodrigues DB (2019) Effects of climate and land-cover changes on soil erosion in Brazilian Pantanal. Sustainability 11(24):7053. https://doi.org/10.3390/su11247053

Cubasch U, Wuebbles D, Chen D et al (2013) Introduction. In: IPCC (ed) Climate change 2013: the physical science basis. Contribution of working group I to the fifth assessment report of the intergovernmental panel on climate change. Cambridge University Press, Cambridge, pp 119–158

Cunha APMA, Zeri M, Leal KD et al (2019) Extreme drought events over Brazil from 2011 to 2019. Atmosphere 10:642. https://doi.org/10.3390/atmos10110642

Dai A, Trenberth KE, Karl TR (1999) Effects of clouds, soil moisture, precipitation, and water vapor on diurnal temperature range. J Clim 12:2451–2473. https://doi.org/10.1175/1520-0442(1999)012%3c2451:EOCSMP%3e2.0.CO;2

Demaria EMC, Rodriguez DA, Ebert EE et al (2011) Evaluation of mesoscale convective systems in South America using multiple satellite products and an object-based approach. J Geophys Res 116:D08103. https://doi.org/10.1029/2010JD015157

Dereczynski C, Chou SC, Lyra A et al (2020) Downscaling of climate extremes over South America—part I: model evaluation in the reference climate. Weather Clim Extremes 29:100273. https://doi.org/10.1016/j.wace.2020.100273

Deser C, Phillips A, Bourdette V, Teng H (2012) Uncertainty in climate change projections: the role of internal variability. Clim Dyn 38:527–546. https://doi.org/10.1007/s00382-010-0977-x

Diffenbaugh NS, Singh D, Mankin JS et al (2017) Quantifying the influence of global warming on unprecedented extreme climate events. Proc Natl Acad Sci 114:4881–4886. https://doi.org/10.1073/pnas.1618082114

Donat MG, Alexander LV, Yang H et al (2013a) Updated analyses of temperature and precipitation extreme indices since the beginning of the twentieth century: the HadEX2 dataset. J Geophys Res Atmos 118:2098–2118. https://doi.org/10.1002/jgrd.50150

Donat MG, Alexander L, Yang H, Durre I, Vose R, Caesar J (2013b) Global landbased datasets for monitoring climatic extremes. Bull Am Meteorol Soc 94:997–1006. https://doi.org/10.1175/BAMS-D-12-00109.1

Drobinski P, Alonzo B, Bastin S et al (2016) Scaling of precipitation extremes with temperature in the French Mediterranean region: what explains the hook shape? J Geophys Res Atmos 121:3100–3119. https://doi.org/10.1002/2015JD023497

Dunn RJH, Alexander LV, Donat MG et al (2020) Development of an updated global land in situ-based data set of temperature and precipitation extremes: HadEX3. J Geophys Res Atmos. https://doi.org/10.1029/2019JD032263

Ehbrecht M, Seidel D, Annighöfer P et al (2021) Global patterns and climatic controls of forest structural complexity. Nat Commun 12:519. https://doi.org/10.1038/s41467-020-20767-z

Escobar GCJ, Reboita MS (2020) Relationship between daily atmospheric circulation patterns and South Atlantic Convergence Zone (SACZ) events. Atmósfera. https://doi.org/10.20937/ATM.52936

Fanourgakis GS, Kanakidou M, Nenes A et al (2019) Evaluation of global simulations of aerosol particle and cloud condensation nuclei number, with implications for cloud droplet formation. Atmos Chem Phys 19:8591–8617. https://doi.org/10.5194/acp-19-8591-2019

Foden WB, Butchart SHM, Stuart SN et al (2013) Identifying the world's most climate change vulnerable species: a systematic trait-based assessment of all birds, amphibians and corals. PLoS ONE 8:e65427. https://doi.org/10.1371/journal.pone.0065427

Frich P, Alexander LV, Della-Marta PM et al (2002) Observed coherent changes in climatic extremes during the second half of the twentieth century. Clim Res 19:193–212. https://doi.org/10.3354/CR019193

National Geographic (2020) South America: physical geography. Web page. https://www.nationalgeographic.org/encyclopedia/south-america-physical-geography/. Accessed 12 Dec 2020

Gettelman A, Rood RB (2016) Demystifying climate models: a user guide to earth system models. SpringerOpen, Boulder

Giorgi F (2010) Uncertainties in climate change predictions, from the global to the regional scale. EPJ Web Conf 9:115–129. https://doi.org/10.1051/epjconf/201009009

Giudicelli GC, Turchetto C, Silva-Arias GA, Freitas LB (2019) Influence of climate changes on the potential distribution of a widespread grassland species in South America. Perspect Plant Ecol Evolut System. https://doi.org/10.1016/j.ppees.2019.125496

Gough CM, Atkins JW, Fahey RT et al (2019) High rates of primary production in structurally complex forests. Ecology 100:e02864. https://doi.org/10.1002/ecy.2864

Gutowski WJ, Giorgi F, Timbal B et al (2016) WCRP coordinated regional downscaling experiment (CORDEX): a diagnostic MIP for CMIP6. Geosci Model Dev 9:4087–4095. https://doi.org/10.5194/gmd-9-4087-2016

Hagemann S, Jacob D (2007) Gradient in the climate change signal of European discarge predicted by a multi-model ensemble. Clim Change 81:309–327. https://doi.org/10.1007/s10584-006-9225-0

Harrison S, Spasojevic MJ, Li D (2020) Climate and plant community diversity in space and time. Proc Natl Acad Sci USA 117:4464–4470. https://doi.org/10.1073/pnas.1921724117

Hartmann DL (2016) Global physical climatology, 2nd edn. Elsevier, Seattle

Hawkins E, Sutton R (2009) The potential to narrow uncertainty in regional climate predictions. Bull Am Meteorol Soc 90:1095–1108. https://doi.org/10.1175/2009BAMS2607.1

Haylock MR, Peterson TC, Alves LM et al (2006) Trends in total and extreme South American rainfall in 1960–2000 and links with sea surface temperature. J Clim 19:1490–1512. https://doi.org/10.1175/JCLI3695.1

Held IM, Soden BJ (2006) Robust responses of the hydrological cycle to global warming. J Clim 19:5686–5699. https://doi.org/10.1175/JCLI3990.1

IPCC (2007) Climate change 2007: the physical science bases. Contribution of working group I to the fourth assessment report of the intergovernmental panel on climate change. Cambridge University Press, Cambridge

IPCC (2010) Good practice guidance paper on assessing and combining multi-model climate projections. In: IPCC expert meeting on assessing and combining multi model climate projections, Boulder

IPCC (2012) Glossary of terms. In: Managing the risks of extreme events and disasters to advance climate change adaptation. A special report of working groups I and II of the intergovernmental panel on climate change. Cambridge University Press, Cambridge, p 1535

IPCC (2013) Climate change 2013: the physical science basis. Contribution of working group I to the fourth assessment report of the intergovernmental panel on climate change. Cambridge University Press, Cambridge

Jimenez JC, Libonati R, Peres LF (2018) Droughts over Amazonia in 2005, 2010, and 2015: a cloud cover perspective. Front Earth Sci 6:227. https://doi.org/10.3389/feart.2018.00227

Khaliq I, Hof C, Prinzinger R et al (2014) Global variation in thermal tolerances and vulnerability of endotherms to climate change. Proc R Soc B 281:20141097. https://doi.org/10.1098/rspb.2014.1097

Khan N, Shahid S, Ahmed K et al (2020) Selection of GCMs for the projection of spatial distribution of heat waves in Pakistan. Atmos Res 233:104688. https://doi.org/10.1016/j.atmosres.2019.104688

Klein Tank AMG, Zwiers FW, Zhang X (2009) Guidelines on analysis of extremes in a changing climate in support of informed decisions for adaptation. World Meteorological Organization, Geneva, p 52

Kreft H, Jetz W (2007) Global patterns and determinants of vascular plant diversity. Proc Natl Acad Sci USA 104:5925–5930. https://doi.org/10.1073/pnas.0608361104

Lang PE, Carslaw DC, Moller SJ (2019) A trend analysis approach for air quality network data. Atmos Environ X 2:100030. https://doi.org/10.1016/j.aeaoa.2019.100030

Latif M (2011) Uncertainty in climate change projections. J Geochem Explor 110:1–7. https://doi.org/10.1016/j.gexplo.2010.09.011

Lázaro WL, Oliveira Júnior ES, Silva CJ et al (2020) Climate change reflected in one of the largest wetlands in the world: an overview of the Northern Pantanal water regime. Acta Limnol Bras 32:e104. https://doi.org/10.1590/s2179-975x7619

Leal Filho W, Azeiteiro UM, Salvia AL, Fritzen B, Libonati R (2021) Fire in paradise: why the pantanal is burning. Environ Sci Policy 123:31–34. https://doi.org/10.1016/j.envsci.2021.05.005

Lee Y, Shin Y, Boo K-O, Park J-S (2020) Future projections and uncertainty assessment of precipitation extremes in the Korean peninsula from the CMIP5 ensemble. Atmos Sci Lett 21:e954. https://doi.org/10.1002/asl2.954

Lemos MC, Lo YJ, Nelson DR et al (2016) Linking development to climate adaptation: Leveraging generic and specific capacities to reduce vulnerability to drought in NE Brazil. Glob Environ Change 39:170–179. https://doi.org/10.1016/j.gloenvcha.2016.05.001

Leutbecher M, Palmer TN (2008) Ensemble forecasting. J Comput Phys 227:3515–3539. https://doi.org/10.1016/j.jcp.2007.02.014

Li J, Chen B, Zhou J, Mo Y (2019) The optimal planning of wind power capacity and energy storage capacity based on the bilinear interpolation theory. In: Yang Q, Yang T, Li W (eds) Smart power distribution systems. Academic Press, pp 411–445

Li S, Otto FEL, Harrington LJ et al (2020) A pan-South-America assessment of avoided exposure to dangerous extreme precipitation by limiting to 1.5 °C warming. Environ Res Lett. https://doi.org/10.1088/1748-9326/ab50a2

Lima AA, Ribeiro MC, Grelle CEV, Pinto MP (2019) Impacts of climate changes on spatio-temporal diversity patterns of Atlantic Forest primates. Perspect Ecol Conserv 17:50–56. https://doi.org/10.1016/j.pecon.2019.04.004

Llopart M, Reboita MS, Coppola E, Giorgi F, da Rocha RP, de Souza DO (2018) Land use change over the Amazon Forest and its impact on the local climate. Water 10(2):149. https://doi.org/10.3390/w10020149

Llopart M, Reboita MS, Rocha RP (2020a) Assessment of multi-model climate projections of water resources over South America CORDEX domain. Clim Dyn 54:99–116. https://doi.org/10.1007/s00382-019-04990-z

Llopart M, Domingues LM, Torma C et al (2020b) Assessing changes in the atmospheric water budget as drivers for precipitation change over two CORDEX-CORE domains. Clim Dyn. https://doi.org/10.1007/s00382-020-05539-1

López-Franca N, Zaninelli PG, Carril AF et al (2016) Changes in temperature extremes for 21st century scenarios over South America derived from a multi-model ensemble of regional climate models. Clim Res 68:151–167. https://doi.org/10.3354/cr01393

Lovino MA, Müller O, Berbery EH, Müller G (2018) How have daily climate extremes changed in the recent past over northeastern Argentina? Glob Planet Change 168:78–97. https://doi.org/10.1016/j.gloplacha.2018.06.008

Loyola RD, Lemes P, Brum FT et al (2014) Clade-specific consequences of climate change to amphibians in Atlantic Forest protected areas. Ecography 37:65–72. https://doi.org/10.1111/j.1600-0587.2013.00396.x

Lyra ADA, Chou SC, Sampaio GDO (2016) Sensitivity of the Amazon biome to high resolution climate change projections. Acta Amazon 46(2):175–188. https://doi.org/10.1590/1809-43922201502225

Lyra A, Tavares P, Chou SC et al (2018) Climate change projections over three metropolitan regions in Southeast Brazil using the non-hydrostatic Eta regional climate model at 5-km resolution. Theoret Appl Climatol 132:663–682. https://doi.org/10.1007/s00704-017-2067-z

Marengo JA, Nobre CA, Sampaio G et al (2011) Climate change in the Amazon basin: tipping points, changes in extremes, and impacts on natural and human systems. In: Bush MB, Flenley JR, Gosling WD (eds) Tropical rainforest responses to climatic change, 2nd edn. Spring, Berlin, pp 259–283

Marengo JA, Liebmann B, Grimm AM et al (2012) Recent developments on the South American monsoon system. Int J Climatol 32:1–21. https://doi.org/10.1002/joc.2254

Marengo JA, Souza CM Jr, Thonicke K, Burton C, Halladay K, Betts RA et al (2018a) Changes in climate and land use over the Amazon region: current and future variability and trends. Front Earth Sci 6:228. https://doi.org/10.3389/feart.2018.00228

Marengo JA, Alves LM, Alvala RCS et al (2018b) Climatic characteristics of the 2010–2016 drought in the semiarid northeast Brazil region. An Acad Bras Ciênc 90:1973–1985. https://doi.org/10.1590/0001-3765201720170206

Marengo JA, Ambrizzi T, Alves LM et al (2020) Changing trends in rainfall extremes in the metropolitan area of São Paulo: causes and impacts. Front Clim. https://doi.org/10.3389/fclim.2020.00003

Marengo JA, Cunha AP, Cuartas LA, Deusdará Leal KR, Broedel E, Seluchi ME et al (2021) Extreme drought in the Brazilian Pantanal in 2019–2020: characterization, causes, and impacts. Front Water 3:13. https://doi.org/10.3389/frwa.2021.639204

Marrafon VH, Reboita MS (2020) Características da precipitação na América do Sul reveladas através de Índices Climáticos. Rev Bras Climatol 26:663–676. https://doi.org/10.5380/abclima.v26i0.72181

Martin GM, Bellouin N, Collins WJ et al (2011) The HadGEM2 family of Met Office Unified Model climate configurations. Geosci Model Dev 4:723–757. https://doi.org/10.5194/gmd-4-723-2011

Martre P, Wallach D, Asseng S et al (2015) Multimodel ensembles of wheat growth: many models are better than one. Glob Change Biol 21:911–925. https://doi.org/10.1111/gcb.12768

Mesinger F, Chou SC, Gomes JL et al (2012) An upgraded version of the Eta Model. Meteorol Atmos Phys 116:63–79. https://doi.org/10.1007/s00703-012-0182-z

Montgomery DC, Jennings CL, Kulahci M (2015) Introduction to time series analysis and forecasting, 2nd edn. Wiley, New Jersey

Montini TL, Jones C, Carvalho LMV (2019) The South American low-level jet: a new climatology, variability, and changes. J Geophys Res Atmos 124:1200–1218. https://doi.org/10.1029/2018JD029634

Moraes RL, Lansac-Toha FM, Schwind LTF et al (2019) Climate change will decrease the range size of snake species under negligible protection in the Brazilian Atlantic Forest hotspot. Sci Rep 9:8523–8536. https://doi.org/10.1038/s41598-019-44732-z

Moss RH, Edmonds JA, Hibbard KA et al (2010) The next generation of scenarios for climate change research and assessment. Nature 463:747–756. https://doi.org/10.1038/nature08823

Mudelsee M (2019) Trend analysis of climate time series: a review of methods. Earth Sci Rev 190:310–322. https://doi.org/10.1016/j.earscirev.2018.12.005

Nobre CA, Marengon JA, Seluchi ME (2016) Some characteristics and impacts of the drought and water crisis in Southeastern Brazil during 2014 and 2015. J Water Resour Prot 8:252–262. https://doi.org/10.4236/jwarp.2016.82022

Oliveira G, Araújo MB, Rangel TF et al (2012) Conserving the Brazilian Semiarid (Caatinga) biome under climate change. Biodivers Conserv 21:2913–2926. https://doi.org/10.1007/s10531-012-0346-7

Oliveira VA, Mello CR, Beskow S (2019) Modeling the effects of climate change on hydrology and sediment load in a headwater basin in the Brazilian Cerrado biome. Ecol Eng 133:20–31. https://doi.org/10.1016/j.ecoleng.2019.04.021

Oliveira RG, Júnior LCGV, da Silva JB, Espíndola DA, Lopes RD, Nogueira JS et al (2021) Temporal trend changes in reference evapotranspiration contrasting different land uses in southern

Amazon basin. Agric Water Manag 250:106815. https://doi.org/10.1016/j.agwat.2021.106815

Parker WS (2013) Ensemble modeling, uncertainty and robust predictions. Wires Clim Change 4:213–223. https://doi.org/10.1002/wcc.220

Parmesan C (2006) Ecological and evolutionary responses to recent climate change. Annu Rev Ecol Evol Syst 37:637–669. https://doi.org/10.1146/annurev.ecolsys.37.091305.110100

PBMC (2013) Sumário Executivo: base científica das mudanças climáticas. Contribuição do Grupo de Trabalho 1 ao Primeiro Relatório de Avaliação Nacional do Painel Brasileiro de Mudanças Climáticas. PBMC, Brasília

PBMC (2020) Base científica das mudanças climáticas. Contribuição do Grupo de Trabalho 1 ao Primeiro Relatório de Avaliação Nacional do Painel Brasileiro de Mudanças Climáticas. PBMC, Rio de Janeiro

Penone C, Allan E, Soliveres S et al (2019) Specialisation and diversity of multiple trophic groups are promoted by different forest features. Ecol Lett 22:170–180. https://doi.org/10.1111/ele.13182

Pesquero JF, Chou SC, Nobre CA, Marengo JA (2010) Climate downscaling over South America for 1961–1970 using the Eta Model. Theoret Appl Climatol 99:75–93. https://doi.org/10.1007/s00704-009-0123-z

Peterson TC, Folland C, Gruza G et al (2001) Report on the activities of the working group on climate change detection and related rapporteurs. World Meteorological Organization, Geneva

Potter C (2004) Predicting climate change effects on vegetation, soil thermal dynamics, and carbon cycling in ecosystems of interior Alaska. Ecol Model 175:1–24. https://doi.org/10.1016/j.ecolmodel.2003.05.004

Rao VB, Franchito SH, Santo CM, Gan MA (2016) An update on the rainfall characteristics of Brazil: seasonal variations and trends in 1979–2011. Int J Climatol 36(1):291–302. https://doi.org/10.1002/joc.4345

Reboita MS, Gan MA, Rocha RP, Ambrizzi T (2010) Regimes de precipitação na América do Sul: uma revisão bibliográfica. Rev Brasil Meteorol 25:185–204. https://doi.org/10.1590/S0102-77862010000200004

Reboita MS, Rocha RP, Dias CG, Ynoue RY (2014a) Climate projections for South America: RegCM3 Driven by HadCM3 and ECHAM5. Adv Meteorol 2014:1–17. https://doi.org/10.1155/2014/376738

Reboita MS, Fernandez JPR, Llopart M et al (2014b) Assessment of RegCM4.3 over the CORDEX South America domain: sensitivity analysis for physical parameterization schemes. Climate Res 60:215–234. https://doi.org/10.3354/cr01239

Reboita MS, Oliveira DM, Freitas CH et al (2015) Anomalias dos padrões sinóticos da atmosfera na América do Sul nos meses de janeiros de 2014 e 2015. Rev Brasil Energias Renov 4:1–12. https://doi.org/10.5380/rber.v4i4.44141

Reboita MS, Rodrigues M, Armando RP et al (2016) Causas da semi-aridez do sertão nordestino. Rev Brasil Climatol 19:254–277. https://doi.org/10.5380/abclima.v19i0.42091

Reboita MS, Marrafon VH, Llopart M, Rocha RP (2018) Cenários de mudanças climáticas projetados para o Estado de Minas Gerais. Rev Brasil Climatol 2018:110–128. https://doi.org/10.5380/abclima.v1i0.60524

Reboita MS, Ambrizzi T, Silva BA et al (2019) The South Atlantic Subtropical Anticyclone: present and future climate. Front Earth Sci. https://doi.org/10.3389/feart.2019.00008

Reboita MS, Reale M, Rocha RP et al (2020) Future changes in the wintertime cyclonic activity over the CORDEX-CORE southern hemisphere domains in a multi-model approach. Clim Dyn. https://doi.org/10.1007/s00382-020-05317-z

Rodrigues PMS, Silva JO, Eisenlohr PV, Schaefer CEGR (2015) Climate change effects on the geographic distribution of specialist tree species of the Brazilian tropical dry forests. Braz J Biol 75:679–684. https://doi.org/10.1590/1519-6984.20913

Rodrigues JAM, Viola MR, Alvarenga LA et al (2020) Climate change impacts under representative concentration pathway scenarios on streamflow and droughts of basins in the Brazilian Cerrado biome. Int J Climatol 40:2511–2526. https://doi.org/10.1002/joc.6347

Rozante JB, Moreira DS, Gonçalves LGG et al (2010) Combining TRMM and surface observations of precipitation: technique and validation over South America. Weather Forecast 25:885–894. https://doi.org/10.1175/2010WAF2222325.1

Rusticicci M, Barrucand M, Collazo S (2016) Temperature extremes in the Argentina central region and their monthly relationship with the mean circulation and ENSO phases. Int J Climatol 37:3003–3017. https://doi.org/10.5380/abclima.v26i0.72181

Salio P, Nicolini M, Zipser EJ (2007) Mesoscale convective systems over Southeastern South America and their relationship with the South American low-level jet. Mon Weather Rev 135:1290–1309. https://doi.org/10.1175/MWR3305.1

Santos DF, Reboita MS (2018) Jatos de baixos níveis a leste dos Andes: comparação entre duas reanálises. Rev Brasil Climatol 14:340–362. https://doi.org/10.5380/abclima.v22i0.47595

Santos DF, Martins FB, Torres RR (2017) Impacts of climate projections on water balance and implications on olive crop in Minas Gerais. Rev Brasil Eng Agrícola Ambient 21:77–82. https://doi.org/10.1590/1807-1929/agriambi.v21n2p77-82

Santos BA, Oliveira MDS, Silva PN et al (2019) Distribuição espaço-temporal dos focos de calor no Estado de Minas Gerais. Anu Inst Geociênc 42:64–84. https://doi.org/10.11137/2019_3_64_84

Sato Y, Goto D, Michibata T et al (2018) Aerosol effects on cloud water amounts were successfully simulated by a global cloud-system resolving model. Nat Commun. https://doi.org/10.1038/s41467-018-03379-6

Scarano FR, Ceotto P (2015) Brazilian Atlantic forest: impact, vulnerability, and adaptation to climate change. Biodivers Conserv 24:2319–2331. https://doi.org/10.1007/s10531-015-0972-y

Schowengerdt RA (2007) Chapter 7—correction and calibration. In: Schowengerdt RA (ed) Remote sensing, 3rd edn. Academic Press, San Diego, pp 285–354

Schulz C, Whitney BS, Rossetto OC et al (2019) Physical, ecological and human dimensions of environmental change in Brazil's Pantanal wetland: synthesis and research agenda. Sci Total Environ 687:1011–1027. https://doi.org/10.1016/j.scitotenv.2019.06.023

Seneviratne SI, Nicholls N, Easterling D et al (2012) Changes in climate extremes and their impacts on the natural physical environment. Managing the risks of extreme events and disasters to advance climate change adaptation. A special report of working groups I and II of the Intergovernmental Panel on Climate Change. Cambridge University Press, Cambridge, pp 109–230

Shafiq Mu, Ramzan S, Ahmed P et al (2019) Assessment of present and future climate change over Kashmir Himalayas, India. Theoret Appl Climatol 137:3183–3195. https://doi.org/10.1007/s00704-019-02807-x

Sillmann J, Kharin VV, Zhang X, Zwiers FW, Bronaugh D (2013) Climate extremes indices in the CMIP5 multimodel ensemble: part 1. Model evaluation in the present climate. J Geophys Res Atmos 118:1716–1733. https://doi.org/10.1002/jgrd.50203

Silva JPR, Reboita MS, Escobar GCJ (2019a) Caracterização da Zona de Convergência do Atlântico Sul em campos atmosféricos recentes. Rev Brasil Climatol 25:355–377. https://doi.org/10.5380/abclima.v25i0.64101

Silva PS, Bastos A, Libonati R et al (2019b) Impacts of the 1.5°C global warming target on future burned área in the Brazilian

Cerrado. For Ecol Manage 446:193–203. https://doi.org/10.1016/j.foreco.2019.05.047

Skansi MM, Brunet M, Sigró J et al (2013) Warming and wetting signals emerging from analysis of changes in climate extreme indices over South America. Glob Planet Change 100:295–307. https://doi.org/10.1016/j.gloplacha.2012.11.004

Skliris N, Zika JD, Nurser G et al (2016) Global water cycle amplifying at less than the Clausius-Clapeyron rate. Sci Rep. https://doi.org/10.1038/srep38752

Soares DB, Lee H, Loikith PC et al (2016) Can significant trends be detected in surface air temperature and precipitation over South America in recent decades? Int J Climatol 37:1483–1493. https://doi.org/10.1002/joc.4792

Souza e Silva JL, Cruz-Neto O, Peres CA et al (2019) Climate change will reduce suitable Caatinga dry forest habitat for endemic plants with disproportionate impacts on specialized reproductive strategies. PLoS ONE 14:e0217028. https://doi.org/10.1371/journal.pone.0217028

Stark SC, Leitold V, Wu JL et al (2012) Amazon forest carbon dynamics predicted by profiles of canopy leaf area and light environment. Ecol Lett 15:1406–1414. https://doi.org/10.1111/j.1461-0248.2012.01864.x

Stark SC, Breshears DD, Aragón A et al (2020) Reframing tropical savannization: linking changes in canopy structure to energy balance alterations that impact climate. Ecosphere 11:e03231. https://doi.org/10.1002/ecs2.3231

Stein A, Gerstner K, Kreft H (2014) Environmental heterogeneity as a universal driver of species richness across taxa, biomes and spatial scales. Ecol Lett 17:866–880. https://doi.org/10.1111/ele.12277

Streck NA, Uhlmann LO, Gabriel LF (2012) Long-term changes in rice development in Southern Brazil, during the last ten decades. Pesq Agrop Brasil 47:727–737. https://doi.org/10.1590/S0100-204X2012000600001

Sun Q, Miao C, Duan Q et al (2017) A review of global precipitation data sets: data sources, estimation, and intercomparisons. Rev Geophys 56:79–107. https://doi.org/10.1002/2017RG000574

Taylor KE, Stouffer RJ, Meehl GA (2012) An overview of CMIP5 and the experiment design. Bull Am Meteorol Soc 93:485–498. https://doi.org/10.1175/BAMS-D-11-00094.1

Tebaldi C, Knutti R (2007) The use of the multi-model ensemble in probabilistic climate projections. Philos Trans R Soc A Math Phys Eng Sci 365:2053–2075. https://doi.org/10.1098/rsta.2007.2076

Titeux N, Henle K, Mihoub J et al (2016) Biodiversity scenarios neglect future land-use changes. Glob Change Biol 22:2505–2515. https://doi.org/10.1111/gcb.13272

Trindade WCF, Santos MH, Artoni RF (2020) Climate change shifts the distribution of vegetation types in South Brazilian hotspots. Reg Environ Change. https://doi.org/10.1007/s10113-020-01686-7

Ummenhofer CC, Meehl GA (2017) Extreme weather and climate events with ecological relevance: a review. Philos Trans R Soc Biol Sci 372:20160135. https://doi.org/10.1098/rstb.2016.0135

Van Vuuren DP, Edmonds J, Kainuma M et al (2011) The representative concentration pathways: an overview. Clim Change 109:5–31. https://doi.org/10.1007/s10584-011-0148-z

Vasquez-Arroyo E, Silva F, Santos A et al (2020) Climate impacts in the Brazilian energy security: analysis of observed events and adaptation options. Sustentabilidade Debate 11:157–196. https://doi.org/10.18472/SustDeb.v11n3.2020.33838

Vera C, Higgins W, Ambrizzi T et al (2006) Toward a unified view of the American monsoon systems. J Clim 19:4977–5000. https://doi.org/10.1175/JCLI3896.1

Vieira RMSP, Tomasella J, Alvalá RCS (2015) Identifying areas susceptible to desertification in the Brazilian Northeast. Solid Earth 6:347–360. https://doi.org/10.5194/se-6-347-2015

Wallach D, Mearns LO, Ruane AC, Rötter RP, Asseng S (2016) Lessons from climate modeling on the design and use of ensembles for crop modeling. Clim Change 139:551–564. https://doi.org/10.1007/s10584-016-1803-1

Walther GR, Post E, Convey P et al (2002) Ecological responses to recent climate change. Nature 416:389–395. https://doi.org/10.1038/416389a

Watanabe M, Suzuki T, Oishi R et al (2010) Improved climate simulation by MIROC5: mean states, variability, and climate sensitivity. J Clim 23:6312–6335. https://doi.org/10.1175/2010JCLI3679.1

Wilks DS (2011) Statistical methods in the atmosphere sciences, 3rd edn. Elsevier, Amsterdam

WMO (1983) Guide to climatological practices, 2nd edn. Secretariat of the World Meteorological Organization, Geneva

Worldometer (2021) Countries in South America by population (2021) United Nations, Department of Economic and Social Affairs, Population Division. https://www.worldometers.info/population/countries-in-south-america-by-population/. Accessed 08 June 2021.

Xavier AC, Ling CW, Scanlon BR (2015) Daily gridded meteorological variables in Brazil (1980–2013). Int J Climatol 36:2644–2659. https://doi.org/10.1002/joc.4518

Xiao-Ge X, Tong-Wen W, Jie Z (2013) Introduction of CMIP5 experiments carried out with the climate system models of Beijing Climate Center. Adv Clim Chang Res 4:41–49. https://doi.org/10.3724/SP.J.1248.2013.041

Zhang X, Aguilar E, Sensoy S et al (2005) Trends in Middle East climate extreme indices from 1950 to 2003. J Geophys Res Atmos 110:D22104. https://doi.org/10.1029/2005JD006181

Zhang X, Alexander LV, Hegerl GC, Klein-Tank A, Peterson TC, Trewin B, Zwiers FW (2011) Indices for monitoring changes in extremes based on daily temperature and precipitation data. Wiley Interdiscip Rev Clim Chang 2:851–870. https://doi.org/10.1002/wcc.147

Zhou J, Lau KM (1998) Does a Monsoon Climate exist over South America? J Clim 11:1020–1040. https://doi.org/10.1175/1520-0442

Zhou L, Dickinson RE, Dirmeyer P et al (2009) Spatiotemporal patterns of changes in maximum and minimum temperatures in multi-model simulations. Geophys Res Lett 36:L02702. https://doi.org/10.1029/2008GL036141

Zilli M, Scarabello M, Soterroni AC et al (2020) The impact of climate change on Brazil's agriculture. Sci Total Environ 740:139384. https://doi.org/10.1016/j.scitotenv.2020.139384

Zou Y, Macau EEN, Sampaio G et al (2016) Do the recent severe droughts in the Amazonia have the same period of length? Clim Dyn 46:3279–3285. https://doi.org/10.1007/s00382-015-2768-x

Zullo Junior J, Pinto HS, Assad ED (2006) Impact assessment study of climate change on agricultural zoning. Meteorol Appl 13:69–80. https://doi.org/10.1017/S135048270600257X

Zullo Junior J, Pinto HS, Assad ED, Evangelista SRM (2008) Potential economic impacts of global warming on two brazilian commodities, according to IPCC prognostics. Embrapa Informática Agropecuária-Artigo em periódico indexado (ALICE). http://www.alice.cnptia.embrapa.br/alice/handle/doc/31863. Accessed 08 June 2021.